ISSN 2582- 564X
AEXTJ
AGRICULTURAL EXTENSION JOURNAL

Available Online at www.aextj.com
Agricultural Extension Journal 2024; 8(3):147-178

RESEARCH ARTICLE

Characterization of Systematic Variations in Met Parameters: Impact of El Nino-Southern Oscillation?

Sazzala Jeevananda Reddy

Former Chief Technical Advisor – WMO/UN and Expert – FAO/UN, Fellow, Telangana Academy of Sciences (Founder Member); Convenor, Forum for a Sustainable Environment

Received: 11-06-2024; Revised: 05-07-2024; Accepted: 31-07-2024

ABSTRACT

In the word "Climate Change," the major component is systematic variations in meteorological parameters such as rainfall, temperature, cyclones, and hurricanes. World Meteorological Organization in 1966 released a manual with the caption "Climate Change." The manual presented methods to analyze the data series such as moving average technique, iterative regression approach, trigonometric approach, and power spectrum method. Studied systematic variations in rainfall (India), temperature (Global, USA, India and Australia), cyclonic storms (India), and hurricanes (USA) and discussed with reference to El Nino Southern-Oscillation (ENSO) factors, Phillippines Typhoons, USA Tornadoes. Indian rainfall at the national level presented 60-year cycle similar to the Telugu Astrological cycle. The river water flows followed this cycle (three rivers, namely, Chinab, Ravi and Bias from North-west India, Bramhaputra River from North-east India and Godavari River from Central-east India). Undivided Andhra Pradesh (AP) rainfall data series and Telangana (TG) Meteorological sub-division rainfall series presented 132-year cycle. TG in addition also presented 58 year cycle. Coastal Andhra (CA) and Rayalaseema meteorological sub-divisions presented in both the Southwest Monsoon (SWM) and Northeast Monsoon seasons 56-year cycle but they presented in opposite phase. The global adjusted average annual temperature data series presented a 60-year cycle with the global warming component of 0.45°C for 1951–2100. However, by replacing the surface data by satellite data, no trend was noted in 2008 by the present author. Later, this satellite data series was deleted from the internet and introduced new data series that showed steep rise in temperature that showed global warming. In fact, satellite data should be lower than the surface data as it accounts oceans that cover around three-forths of global area and rural-cold-island effects part that forms a major part of one-fourth of land surface area; that helped bringing down the temperature and thus the global warming trend must be nearly zero. Indian temperature presented typical patterns. Maximum temperature series presented a depression that followed above the average part of 60-year cycle of All-India average annual rainfall (1927/28–19567/57). However, with the lesser degree, this is also reflected in the mean annual and mean annual minimum temperatures. The Australian surface air and sea surface temperatures presented 120-year cycle with zero trend and thus zero global warming for 1951–2100 with the starting and the ending parts presenting extremes. The Bay of Bengal cyclones followed 56-year cycle of SWM season CA met sub-division with no trend. USA hurricanes presented 60-year cycle but presented an increasing trend unlike Bay of Bengal cyclones. Tornadoes confined to one part of the USA and Typhoons confined to one part of the Philippines. ENSO showed no impact on systematic variations.

Key words: Characterization, climate change, cyclones, El Nino-southern oscillation, hurricanes, rainfall, systematic variations, tornadoes, temperature, tphoons

Address for correspondence:
Sazzala Jeevananda Reddy
E-mail: jeevananda_reddy@yahoo.com

INTRODUCTION

Mitchel *et al*.[1] brought out a manual on "Climate Change" prepared by eminent Meteorologists from

National Meteorological Departments – Late Shri K.N.Rao from Indian Meteorological Department (IMD) is one of the author. To separate trend from natural variability, the manual suggested methods such as "the Moving Average Technique, the Iterative Regression Approach, the Trigonometric Functions, the Power Spectral Analysis of Blackman and Tukey,[2] etc." The major hurdle in this study is the availability of long-term continuous data series. In the case of temperature, major part is adjusted data series only.

The author started applying moving average technique as back as 1975 after collecting the dates of onset of South-west Monsoon (SWM) from the daily, weekly, and monthly weather reports of IMD. Reddy[3] brought out the publication using moving average technique with the dates of onset of SWM over Kerala Coast. From this, it is forecasted that 2004 onset of SWM over Kerala will be early. BRMS[4] applied to temperature for 10, 30, and 60-year moving averages to eliminate trend and thus identification of natural cycle (60-year cycle). Using the method of Blackman and Tukey,[2] Reddy *et al*.[5] analyzed total (global) solar radiation from the sun and net radiation balance from the earth. The total and net radiation balance data series were computed using the models of Reddy,[6-10] Reddy and Rao.[11] In the majority of the cases, applied iterative regression approach – Reddy and Singh[12] analyzed the rainfall data of Mahalapye in Botswana. The power spectrum technique was used by Parthasarathy and Mooley,[13] Reddy *et al*.,[5] Reddy[14] etc.

The analysis was carried out for rainfall (India), temperature (India, Australia, USA and Global), Cyclones in Bay of Bengal, and Hurricanes in USA. These are discussed in relation to El Nino-Southern Oscillation (ENSO) and presented general discussion on typhoons in Philippines and tarnidoes in USA.

CHARACTERIZATION OF SYSTEMATIC VARIATIONS IN MET PARAMETERS: ANALYSIS PROCEDURES

Introduction

Let me present a few basics relating to meteorological parameters (Reddy[15]) such as rainfall. The data were based on IMD climate normals of 1961–1990 and Parthasarathy *et al*.[16]

Table 1 presents the lowest and the highest rainfall amounts and their year of occurrence during 1871–1994; Table 2 presents average rainfall in each part of the cycle during SWM – June to September and Northeast Monsoon (NEM) – October to December to understand climate cyclic pattern.

Table 3 presents the mean and coefficient of variations for India, Coastal Andhra (CA), Rayalaseema (RS) and Telangana (TG) rainfall. Table 4 presents the SWM and NEM rainfall % years with <90% of average and Cyclonic activity in Bay of Bengal Statistics.

These four tables presented high variability for All-India and undivided Andhra Pradesh (AP) that comprises of three meteorological sub-divisions, namely, CA, RS and TG.

Analysis Procedure: An Example

For the identification of climate fluctuations in rainfall data, one needs long and continuous

Table 1: The lowest and the highest rainfall amounts and their year of occurrence during 1871–1994

Period	The lowest		The highest	
	Mm	Year	Mm	Year
Coastal Andhra				
Annual	532.0	1891	1501.5	1990
SWM	308.5	1888	780.3	1978
NEM	87.9	1909	702.7	1994
Rayalaseema				
Annual	223.7	1876	1228.3	1874
SWM	193.4	1904	791.9	1878
NEM	12.0	1876	455.5	1946
Telangana				
Annual	489.0	1920	1485.2	1893
SWM	371.4	1877	1186.0	1988
NEM	2.0	1988	309.8	1987

Table 2: Average rainfall in each part of the cycle (28-years) during SWM and NEM

Period	Seasons					
	SWM			NEM		
	CA	RS	TG	CA	RS	TG
	Average rainfall, mm					
1871–1888*	477.2	428.2	641.3	425.0	232.6	106.9
1889–1816	509.2	431.9	743.1	330.0	186.7	090.7
1917–1944	477.3	386.1	673.2	409.6	204.5	104.4
1945–1972	531.6	423.8	761.8	356.0	197.7	107.6
1973–1994*	528.7	429.9	753.4	395.4	205.1	134.0

*Full cycle years data is not available

records. The climate fluctuations form part of the natural/systematic/rhythmic/cyclic variability component of "climate change" in meteorological parameters. To understand the natural variability, carried out analysis of the rainfall and temperature and cyclones and hurricanes data series of different countries/locations. The iterative autoregression approach was used in majority of the cases (Reddy[17]). Some of these relating to rainfall, solar, and net radiation intensities are presented below:

Using moving average technique analyzed the Indian onset dates of SWM data and observed 52-year cycle (Reddy[3]); Using iterative regression approach analyzed Mahalapye in Botswana rainfall data and observed 60-year cycle (Reddy and Singh[12])*; Using the power spectrum method of Blackman and Tukey[2] analyzed the data series of global solar radiation from the sun and the net radiation from the Earth and observed 11 (10.5 ± 0.5) year sunspot cycle (Reddy *et al*.[5]); Using the power spctrum method of Blackman and Tukey[2] analyzed the northeast Brazil rainfall data series and observed 52-year cycle (Reddy[14]); Using iterative regression approach analyzed the rainfall data of Mozambique (Zimbabwe and Malawi) and observed 54 and 18 and 40 year cycles (Reddy[18])*; Using iterative regression approach analyzed the rainfall data of Ethiopia and observed principally 28 and 38-year cycles (also presented 40 and 56 year cycles) with the Asmara in Eritrea presenting 22-year cycle (Reddy and Mersha[19])*.

Using the iterative regression approach analyzed the rainfall data of all India annual average rainfall (Reddy[20]) and observed 60-year cycle; and also for the SWM average rainfall (Reddy[15]) observed 60-year cycle*. Using iterative regression approach analyzed the annual, SWM and NEM rainfall series of undivided AP and it's three met sub-divisions, namely, CA, RS and TG that presented 132 and 56-year cycles (Reddy[15,21])*.

Table 3: Mean and CV of rainfall based on the data of 1871–1990 (mm)

Region	Parameter	SWM	NEM	Annual
India	Mean, mm	852 (78)	120 (11)	1090
	CV%	09.9	29.0	19.5
TG	Mean, mm	722 (80)	197 (12)	899
	CV%	23.5	60.3	21.7
RS	Mean, mm	422 (60)	204 (29)	709
	CV%	28.8	41.9	21.6
CA	Mean, mm	507 (52)	375 (39)	970
	CV%	22.2	38.8	19.8

CA: Coastal Andhra, RS: Rayalaseema, TG: Telangana, SWM: Southwest Monsoon, NEM: Northeast monsoon, CV: Coefficient of variation, numbers within the brocket refer to % of rainfall

Table 4: SWM and NEM rainfall % years with <90% of average and cyclonic activity in Bay of Bengal statistics

Period	Rainfall (% years with <90% In 28 year periods)						Cyclones in Bay of Bengal (of average) (May to November) $ Number
	SWM			NEM			
	CA	RS	TG	CA	RS	TG	
1861–1888*	72	61	72	33	28	66	<10
1889–1916	53	43	46	60	71	71	>10
1917–1944	75	78	68	46	50	60	<10
1945–1972	43	43	32	64	60	46	>10 (10–16)
1973–2000**	54	54	54	41	45	41	<10 (0–8)
2001–2027 and	<50	<50	<50	>50	>50	>50	>10

*1871–1888, **1973–1994, average cyclones 10, SWM: Southwest monsoon, NEM: Northeast monsoon, CA: Coastal Andhra, RS: Rayalaseema, TG: Telangana met sub-divisions, $: Joint typhoon warning center – Bay of Bengal Region Cyclones per year during 1945–2000 (May-November) and projected

Estimation of amplitude and phase angles using trigonometric method

To be useful for the prediction of long-term patterns, synthesized curve of the observed periodicities has to be determined. This can be achieved through a trigonometric function (Reddy[17]; Mitchel *et al*.[1]). In Table 5 presented, the estimates of cycles in years, amplitudes in mm, and the respective phase angles in degrees of the sign curve derived using trigonometric approach and integrated curves were derived and given in Figure 1a and b for Catuane in Mozambique are based on cycles 54 years and its sub-multiple 18 years; and in the case of Durban in South Africa, it is based on 66 year and its sub-multiple of 22-year cycles.

Maputo and Beaira rainfall followed Catuane [Table 5] pattern of 54 and 18-year cycles. The three

Table 5: Estimates of cycle in years, amplitude in mm, and phase angle in degrees

Catuane			Durban		
T_k	A_k	ϕ_k	T_k	A_k	ϕ_k
(Years)	(mm)	(Degrees)	(Years)	(mm)	(Degrees)
54	200	86.7	66	250	185.5
18	200	100.0	22	350	180.0

T_k: Cycle period in years, A_k: Cycle amplitude in mm, ϕ_k: Phase angle in degrees

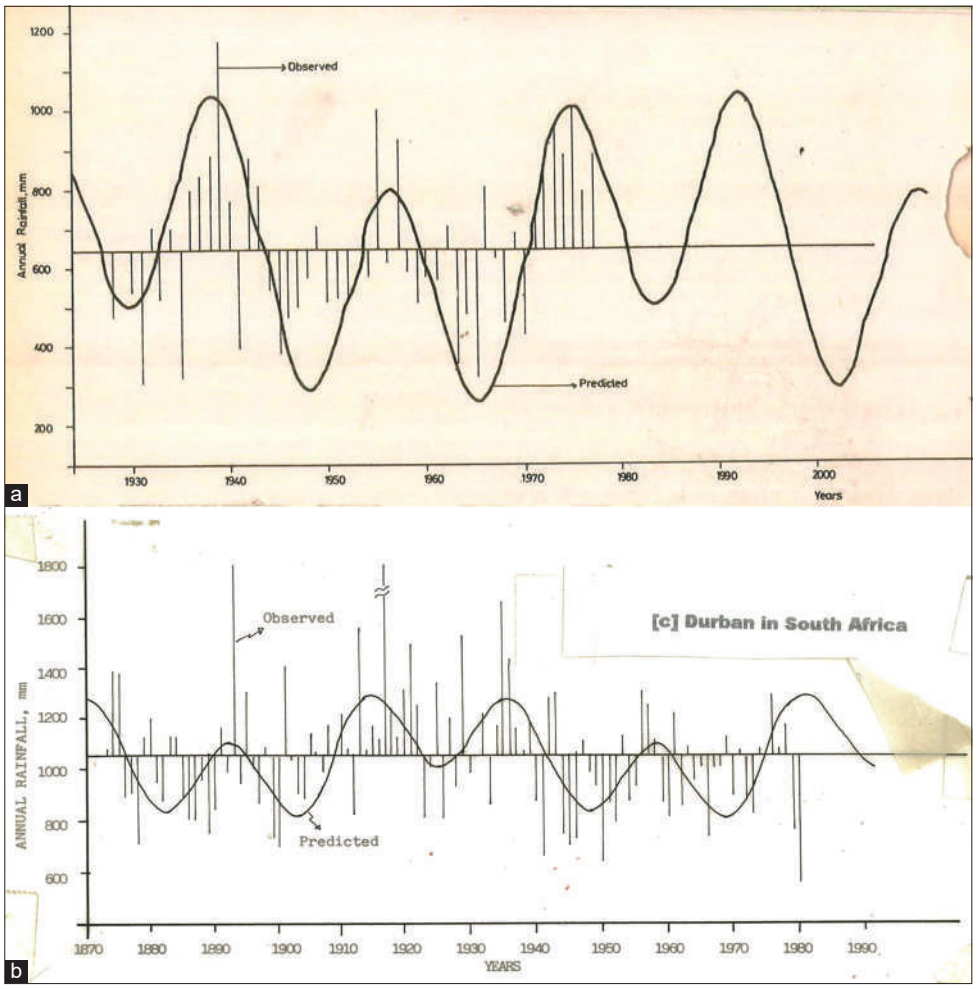

Figure 1: (a) Observed and predicted pattern of Catuane rainfall (Source: Reddy, 1986), (b) Observed and predicted pattern of Durban rainfall (Source: Reddy, 1986)

stations presented low, medium, and high rainfall conditions. The integrated pattern of below average and above average patterns followed "M" and "W" shape [Figure 1a and b] -- with the central part of W and M present opposite part of the cyclic pattern --, respectively, followed above the average and below the average parts of the cycle. The same is the case with the Durban with medium rainfall. These are given in Table 6 and for one cycle presented predictive estimates (+ means above the average and - means below the average).

CHARACTERIZATION OF SYSTEMATIC VARIATIONS IN INDIAN RAINFALL

Introduction

Indian rainfall is associated with the monsoons systems. The word "Monsoon" owes its origin to an Arabic word meaning "season." It was used by seamen, several centuries ago, to describe a system of alternating winds over the Arabian Sea. However, on the precise definition of the Monsoon, there is disagreement among scientists. With all the disagreements it is a fact that the term is used connote a seasonal wind, which blows with consistency and regularity during a part of the year, and which is absent or blows from another direction for the rest of the year (Reddy[15]). The former relates to the winds blowing from the South-west and is termed as the SWM "around" June to September. This is also known as summer monsoon and Kharif season. The later relates to the winds blowing from the Northeast and is termed as the North-east Monsoon (NEM) "around" from October to December. This is also termed as winter monsoon and Rabi season.

Table 6: Natural variability in rainfall "predictive cases" of catuane, maputo, beira in mozambique and Durban in South Africa

Catuane, Maputo, Beira and Durban information					
Station	**Average rainfall (mm)**		**Cycle 1**	**Cycle 2**	**Cycle 3**
Catuane	Low	(620)	1943–1996	1997–2050	2051–2104
Maputo	Medium	(900)	1925–1978	1979–2032	2033–2086
Beira	High	(1480)	1931–1984	1985–2038*	2039–2092
Cycle 2 of Beira (54 and 18 years cycles integrated output)					
	W=1985–1995(-)			1996–2000(+)	2001–2011(−)
	M=2012–2022(+)			2023–2027(-)	2028–2038(+)
Durban	Medium	(1050)	1876–1942	1943–2009	2010–2075
Cycle 3 of Durban [66 and 22 years cycles integrated output]					
	W=2010–2023(-)			2024–2028(+)	2029–2042(−)
	M=2043–2056(+)			2057–2061(-)	2062–2075(+)

+Above the average, −below the average, W: Shape of below the average, M: Shape of above the average part of respective cycles

Data Availability

The data series were taken from Parthasarathy *et al*.[16] report "Monthly and seasonal rainfall series for All-India homogeneous regions and meteorological (Met) sub-divisions for 1871–1994." The rainfall averages were computed for three met sub-divisions, namely, CA, RS, and TG for both the SWM and the NEM seasons and from met sub-divisions data series estimated annual values for the undivided AP. To create data series for long years for "all-India annual average rainfall," in addition to Parthasarathy *et al*.,[16] data series of 1871–1872–1983–1984 for June to May (computed) added the data series of 1984–1985–2014–2015 for June to May that was taken from the Central Water Commission report.

Data Analysis and Discussion

All-India rainfall

SWM season annual average rainfall

The all-India SWM seasonal annual averages rainfall that constituted 78.2% of the annual, a new data series of SWM period at 10-year averages was created from the data of Parthasarathy *et al*.[16] Ten-year averages were plotted for 1871–1900 and this showed a simple sine curve with 60-year cycle. 1871–1900 and 1931–1960 are above the average 30-year periods and 1901–1960 and 1961–1990 are below the average 30-year periods. The current above the average part of the cycle started around the year 1991 and will continued up to around the year 2020. Expected below the average SWM rainfall during 2021–2050, that is, in the majority of the coming 30-year period (Reddy[15]). This is corrected with all-India annual average rainfall for correct start and end for 30-year periods.

All-India annual average rainfall

Reddy[20] presented Figure 2 using the annual average rainfall of June to May for the period 1871-1872–2014-2015. The figure presented 60-year cycle. This pattern followed the Telugu Astrological cycle of 60 years and the Chinese Astrolocal 60-year cycle but lagging by 3 years to the Telugu Astrological cycle. The current cycle started in 1987–1988 (Prabhava year) and ended above the average 30 years part by 2016–2017 in all-India annual average rainfall. The below the average part commenced in the year 2017–2018 and is expected to end by 1946–1947. Two full 60-year cycles completed and in the case of the third cycle, the 30-year above the average part completed and started below the average 30-year part. River water flows followed this pattern [Figure 2], let us see three cases in the next section:

Undivided AP rainfall

AP average annual rainfall [Figure 3a and b]

AP as a whole and separately the three met sub-divisions, however, do not follow the all-India rainfall pattern [Figure 2]. Reddy[15,21] analyzed the undivided AP rainfall. The three met sub-divisions, namely, CA, RS and TG rainfall series were added to get AP rainfall. AP average annual rainfall

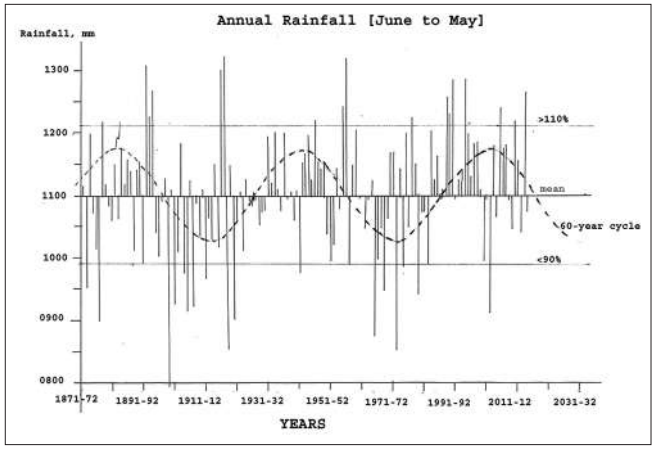

Figure 2: The annual march of all-India rainfall (June–May) from 1871–1872 to 2014–2015 (vertical lines are rainfall observed and dotted curve present 60-year cycle)

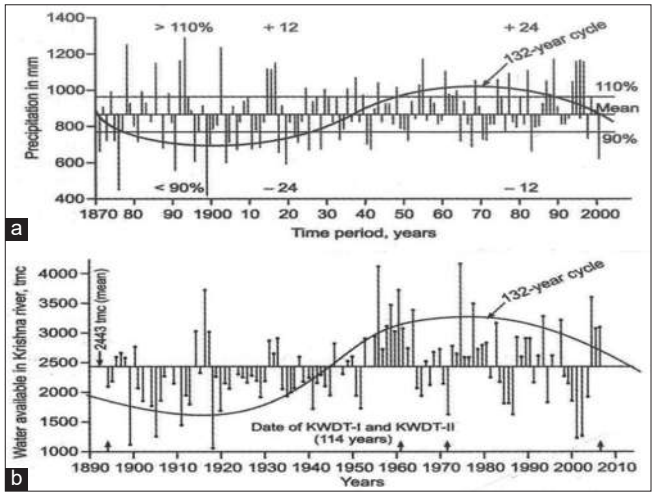

Figure 3: (a) Andhra Pradesh rainfall and (b) Krishna river water flows

presented 132-year cycle [Figure 3a]. One cycle completed by 2001 and commenced a new 132-year cycle starting with the below the average part of the cycle. In the case of below the average 66-year period, in 24 years, it presented deficit rainfall and in 12 years surplus rainfall and the rest comes under normal rainfall years. In the case of above the average 66-year period, in 24 years, it was presented surplus rainfall, and in 12 years deficit rainfall years and the rest normal rainfall years.

AP CA met sub-divisional rainfall [Figure 4]

Presented the CA met sub-divisional SWM and NEM Rainfall pattern of 5-year averages (solid line) along with 56-year cycle (dotted lines). SWM pattern is simply a mirror image to NEM pattern,

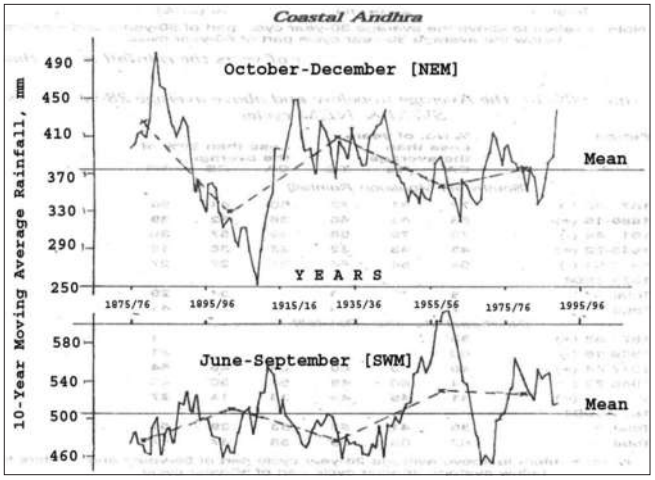

Figure 4: Coastal Andhra met sub-division Southwest monsoon and Northeast monsoon rainfall: Observed (10-year moving averages) and predicted 56-year patterns

that is, NEM 56-year cycle is a mirror image of SWM 56-year cycle.

AP TG met sub-divisional average rainfall [Figure 5]

Presents the 132-year and 58-year cycles. The NEM rainfall is insignificant. In the figure, the solid curve presents the 132-year cycle and dotted curve presents the 58-year cycle. The red color represents below the average pattern and the green color represents above the average patterns.

Rivers water flows

Water flows in the three northwestern rivers (Chenab, Ravi, and Beas)

Table 7 presents the frequency of occurrence of floods in three North-west Indian rivers, namely, Chenab, Ravi, and Beas. The data are arranged under below the average and above the average periods. It was found that one in nine, one in 14, and one in 8 years the frequency of occurrence of floods in Chenab, Ravi and Beas, respectively, are in below the average cycle part; and 1 in 3, 1 in 3, and 1 in 2 years the frequency of occurrence of floods in Chenab, Ravi, and Beas, respectively, are in above the average cycle part Figure 2. These data were taken from "State of Environment Report, India – 2009, MoEF/GoI" and it stated that the frequency of floods in India is largely due to deforestation in the catchment area, destruction of surface vegetation, changes in land use, increased urbanization, and other developmental activities. This is an inaccurate

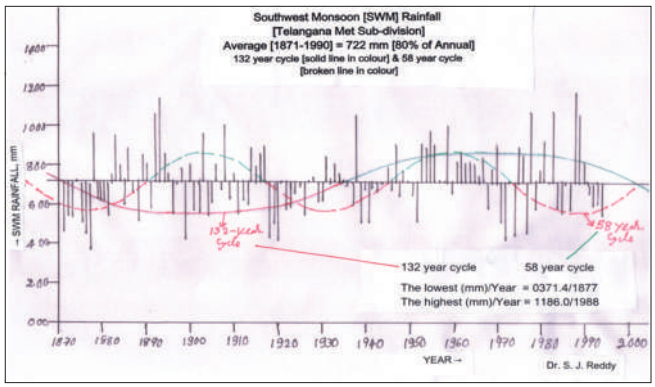

Figure 5: Telangana met Sub-division Southwest monsoon rainfall: observed and predicted patterns

statement as the frequency of occurrence of floods is more frequent from 1990 and less frequent before 1990 [Figure 2].

Brahmaputra river water flows [Figure 6]

Rao *et al*. -- "Seven centuries of reconstructed Brahmaputra river discharge demonstrate underestimated high discharge and flood hazard frequency," Nature Communications volume 11, Article number: 6017 (November 26th, 2020). They used seven-century (1309–2004 C.E) tree-ring data for the reconstruction of monsoon season Brahmaputra discharge. According to this, 1957–1958–1986–1987 ranks among the driest of the past seven centuries (13th percentile) -- this is the below the average 30 year periods in all-India annual rainfall [Figure 2]; also 1830–1860 tree ring part of dry period fall under below the average 30-year period (1837–1838–1866–1867) of all-India annual average rainfall. Figure 2 presents the river path of the tree ring study.

In the executive summary, the authors said: Here, we use a new seven-century (1309–2004 C.E) tree-ring reconstruction of monsoon season Brahmaputra [Figure 6] discharge to demonstrate that the early instrumental period (1956–1986 C.E.) ranks among the driest of the past seven centuries (13th percentile) – this matches with the 60-year cycle in all India annual average rainfall --; Flood hazard inferred from the recurrence frequency of high discharge years is severely underestimated by 24–38% in the instrumental record compared to previous centuries and climate model projections. A focus on only recent observations will therefore be insufficient to accurately characterize flood hazard risk in the region, both in the context of natural variability and climate change – It is the hypothetical statement and untrue.

Table 7: Frequency of occurrence of floods in three northwest Indian Rivers

Frequency of high-magnitude floods			
River	**Period**	**Frequency**	**Climatic**
Chenab	1962–1990	1 in 9 years	(a)
	1990–1998	1 in 3 years	(b)
Ravi	1963–1990	1 in 14 years	(a)
	1990–1998	1 in 3 years	(b)
Beas	1941–1990	1 in 8 years	(a)
	1990–1995	1 in 2 years	(b)

a=below the average cycle, b=above the average cycle [Figure 2], &State of Environment Report, India – 2009, MoEF / GoI: The frequency of floods in India is largely due to deforestation in the catchment area, destruction of surface vegetation, changes in land use, increased urbanization and other developmental activities

Godavari river water flows

Figure 7 presents the water flows in Godavari river. The data were taken from the Bachawat tribunal award report on Godavari river. The data series cover one full cycle (60-years) period. The central part covers below the average part of 30 years and above the average 30-year period is covered on either side. The difference in mean water flows during above and below the averages showed 650 tmc ft [Figure 2].

Krishna river water flows

Figure 3b presented the river Krishna water flow pattern. The vertical lines representing water flows taken from Bachawat tribunal award and solid curve represents the 132-year cycle taken from Figure 3a. In the case of water flows in the river Krishna during deficit 66 years only 12 years showed little surplus water and in the case of above the average 66-year period around 21 years showed deficit years [Figure 3b]. The rainfall showed an increase after the year 1951. It is pertinent to note that before 1957, the data were recorded in inches and after 1957, they were measured in millimeters. However, the increase in rainfall seen in the case of AP after 1950s may not be associated to this shift in recording of data. Water inflows during the below the average rainfall period from 2001 into Srisailam dam were as follows: 361, 111, 13, 12, 23,1273, --, --, --, 411, 209, 055, 853.52, 632.25,

Figure 6: Tree rings study (1309–2004) zone

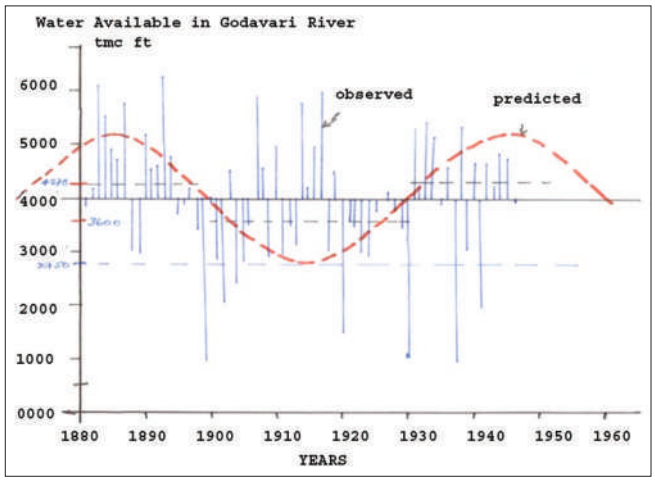

Figure 7: Water availability in Godavari river -- the all-India annual rainfall pattern

71.01, 351.77, 410.00, 584.34, 1786,67, 1785.59, 1102.43, 2039.87, 144.36 by 2023-24 in tmc ft with the maximum capacity of 850 tmc ft. That means in 15 years were below the average and 5 years were above the average. The water entered the Sea from 2013-2014–2021-2023 were 599, 73, 9.21, 55.00, 0.00, 39.30, 797.12, 1278.12, and 153.921 tmc ft.

CHARACTERIZATION OF SYSTEMATIC VARIATIONS IN TEMPERATURES

Introduction

Different regions of the world warm at different rates. It is also different between the Hemispheres. The Northern Hemisphere (NH) warm much faster than that of the Southern Hemisphere (SH). This is basically because more land area and less ocean area in the NH and less land area and more ocean area in the Southern Hemisphere. General circulation pattern (Western Disturbances in India and Jet Steams in USA) plays an important role in the modification of temperatures. The oceans and their marginal seas cover nearly three-quarters (70.8%) of the Earth's surface and the exposed land occupied the remaining one-quarter (29.2%). The cold-island effect plays an important role in reducing the temperature in rural land areas.

Lacunae in temperature data in terms of space and time (limitations -- NOAA)

The term temperature anomaly means a departure from a reference value or long-term average. A positive anomaly indicates that the observed temperature was warmer than the reference value, while a negative anomaly indicates that the observed temperature was cooler than the reference value. The United Nations Intergovernmental Panel on climate change (IPCC) says global temperature is expected to reach or exceed 1.5°C of warming on an average over the next 20 years. Figure 8a presents the time series of observations network and years for USA. The surface measurements reduced with the inclusion of satellite data.

Absolute estimates of global average surface temperature are difficult to compile for several reasons. Some regions have few temperature

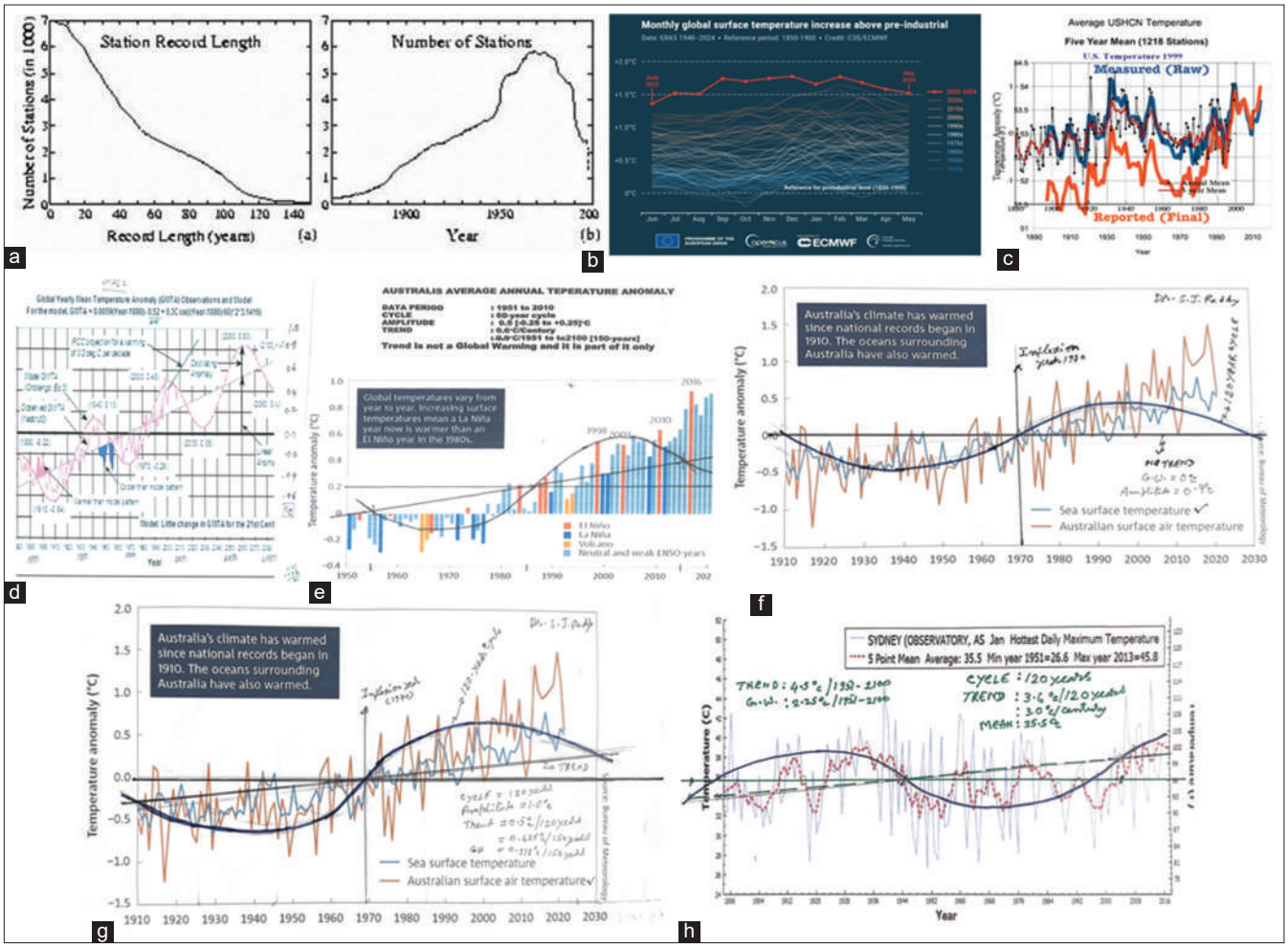

Figure 8: (a) The accuracy of the temperature anomaly primarily relates to met data network (ocean data scenario is very poor), (b) monthly global surface air temperature anomalies (°C) relative to 1850–1900, from January 1940 to May 2024, plotted as time series for each year spanning June to May of the following year. /Credit: C3S/ECMWF, (c) average USHCN annual temperature of raw data series and superposed on it the 5-year mean of 1218 stations (measured) and adjusted data (below red pattern), (d) the global average annual temperature anomaly for the period 1880–2010, along with 60-year cycle pattern, (e) presents Australian mean annual temperature anomaly data for 1950–2020 presenting 60-year cycle with the inflexion point year as 1985, (f) presented australian mean annual sea surface temperature anomaly – the curve is of 120-year cycle, (g) australia's mean annual surface air temperature Anomaly, (h) Sydney's (observatory) hottest daily maximum temperature – (vertical lines) and 5 point mean (red dots) and 120-year cycle (solid curve) – dotted line trend but real trend is "zero trend solid line"

measuring stations (e.g., the Sahara Desert, Thar Desert, etc.) and interpolation must be made over large, data-sparse regions. In mountainous areas, most observations come from the inhabited valleys, so the effect of elevation on a region's average temperature must be considered as well. For example, a summer month over an area may be cooler than average, both at a mountaintop and in a nearby valley, but the absolute temperatures will be quite different at the two locations. The use of anomalies in this case will show that temperatures for both locations were below average.

Using reference values computed on smaller (more local) scales over the same time period establishes a baseline from which anomalies are calculated. This effectively normalizes the data so they can be compared and combined to more accurately represent temperature patterns with respect to what is normal for different places within a region. For these reasons, large-area summaries incorporate anomalies, not the temperature itself. Anomalies more accurately describe climate variability over larger areas than absolute temperatures do, and they give a frame of reference that allows more

meaningful comparisons between locations and more accurate calculations of temperature trends. This type of anomalies has major deficiency.

The global maps show temperature anomalies relative to the 1991–2020 base period. This period is used to comply with a recommended World Meteorological Organization (WMO) Policy, which suggests using the latest decade for the 30-year average – this has no meaning as IMD 30-year normal change for every 30-year period, for example, 1931–1960, 1961–1990, 1991–2020, etc. Nowhere WMO said this. These are only latest climate normals only. This creates more errors by changing the anomaly with the changing normal period. IPCC specified 1951 as the starting year of global warming. We do not have accurate covering in terms of space and time over oceans/seas and rivers, dams, etc. That means it should be compared with data averages before 1951.

The land and ocean gridded dataset is a large file (~24 mb) that contains monthly temperature anomalies across the globe on a 5 deg × 5 deg grid. The anomalies are calculated with respect to the 1991–2020 base period. Gridded data is available for every month from January 1850 to the most recent month available. You can use it to examine anomalies in different regions of the Earth on a month-by-month basis. The index values are an average of the gridded values; however, the global temperature anomalies are provided with respect to the 20th century (1901–2000) average. They are most useful for tracking the big-picture evolution of temperatures across larger parts of the planet, up to and including the entire global surface temperature. This type of usage itself added more bias in the estimation of global warming. Figure 8b presents the scatter of June to May yearly averages overlapping. June to May with NH winter months and SH Summer months presenting higher values during the SH summer months which cover more ocean area and less land area in SH and covers more land area and less ocean area in NH --- relative to 1850–1900, from January 1940 to May 2024, plotted as time series for each year spanning June to May of the following year./Credit: C3S/ECMWF.

Discussion

USA and global mean annual temperatures

Figure 8c presents the USHCN Annual Average observed and adjusted temperature data series. On the observed (raw) data superposed the 5-year mean of 1218 stations. The adjusted data presented below in red pattern. In the raw data (unadjusted), no trend is observed, but unadjusted data presented a trend. Both the data sets presented 60-year cycle.

The natural variability part of the adjusted global average annual temperature of the ocean surface temperatures and the land surface air temperature for 1880–2010 is given in Figure 8d. It presented 60-year cycle similar to Figure 8c of the USA data (adjusted and unadjusted). It varied between −0.3 and +0.3°C (sine curve [cycle] Amplitude is 0.6°C). The trend presented 0.6°C per century. IPCC proposed more than half of the trend is the greenhouse effect part and in this major component is global warming starting from 1951 [IPCC proposed 1951 as the starting year of the global warming. If we take global warming component as 50% of the total trend then the global warming is 0.45°C for 1951–2100. The trend for 1850–2100 is 1.34°C and thus the global warming component is 0.40°C. Less than half is the non-greenhouse effect part, that is, it covers land use and land cover changes. Inflection point year is 1985 – inflection point refers to the change from below the average to the above average.

Australian mean annual temperatures

Mean annual temperature

Figure 8e presents Australia's mean annual surface air temperature anomaly data for 1950–2020. It presented a 60-year cycle and the inflexion point year is 1985. The amplitude of the cycle is varied between −0.30 and +0.30 (cycle amplitude is 0.6°C). The trend is 0.6°C per century. 50% of the trend is global warming, i.e., 0.3°C per century. The global warming for 1951-2100 [i.e., for 150 years] is 0.45°C. Here, the data are for 75 years only and the cut of values on either side are not following the 60-year cycle pattern thus it suggests that it should be longer than 60-year cycle. This is clear from Figure 8f and 8g, wherein they presented 120-year cycle. The Figure 8e includes events such as El Nino, La Nina, Neutral -- weak ENSO years and Volcano years. The temperature varied from year to year. Increasing surface temperatures are seen even in La Nina year which is warmer than an El Nino year. However, the impact of ENSO and Volcanic activity on temperature is not clearly seen.

Mean annual surface air and sea surface temperatures

In Figures 8f and 8g presented bureau of meteorology graph demonstrating how Australia's climate has warmed since national records began in 1910. The author constructed cyclic patterns and global warming, given as: In Figures 8f and 8g the mean annual sea surface and surface air temperatures series presented 120-year cycles; and presented 1972 as inflection year; and presented "zero" global warming with the extremes in the last; The cycle amplitudes presented 1.00 (−0.5–+0.5)°C and 0.90 (−0.45–+0.45)°C. The SH global warming appears to be less than the average and thus less than the NH part of the global warming. It means the average global warming overestimate for SH and underestimate for the NH. Similar pattern is seen in carbon dioxide quantity where in it is less than that of NH.[22]

Sydney's hottest daily maximum temperature

Figure 8h presented the Sydney (observatory) hottest daily maximum temperature for 1894–2018 with 5 5-point mean average 35.5°C; minimum year 1951 it is 26.6°C; and maximum year 2013 it is 45.8°C.

Figure 8h presented 120-year cycle with no trend like sea surface and surface air temperatures but with the inflection point at 1945 instead of 1972; In the Figure 8g the author tried to fit to the trend [Figure 8f] but it is not following the cyclic pattern properly due to sudden jump at the end; by joining the trend dotted line with zero trend solid line (see markings with dots on the solid line), we got clear cut 120-year cycle; However, within the 120 years cycle short term fluctuations are seen; The below the average part of the Sydney's 120-year cycle started in1945 and ended by 2005; The above the average part started in 1885 – a shift of 25 years backward in inflection point years (1972–1945). Furthermore, the 120 year cyclic pattern presented in opposition to sea surface temperature 120-year cyclic pattern with a shift of 25 years.

Indian temperatures

Figure 9a presents the average annual maximum temperature of India for 1880–2020. It presented a depression (D) around 1931–1960. The D is associated with the rainfall cycle of 60-years [Figure 2] wherein 1931–1960 is above the average rainfall cycle with on either side of the D showed

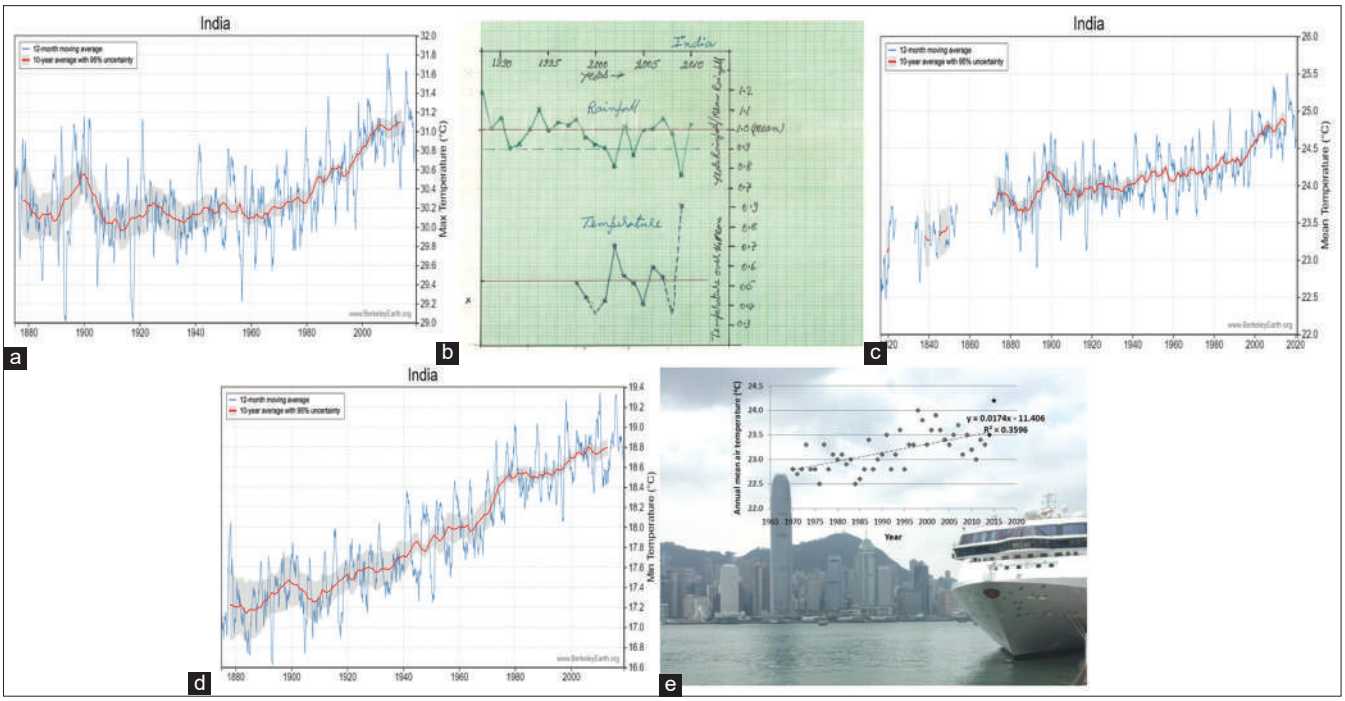

Figure 9: (a) Indian annual mean maximum temperature (Source: IMD). (b) India: Annual precipitation versus annual temperature, (c) Indian annual mean temperature of India (Source: IMD), (d) Indian annual mean minimum temperature (Source: IMD), (e) Presents the Urban-Heat-Island-Effect for Hong Kong – a linear increase with considerable year-to-year variations

increasing pattern in association with drought conditions [Figure 2]. This is seen in Figure 9b -- It presented the variation of Indian annual average rainfall (top) with Indian average annual temperature (bottom) wherein 2002 and 2009 are drought years with decreased mean annual rainfall presented increased mean annual temperature.

Figure 9c presents the mean annual average temperature increasing pattern with the lower D impact of Figure 9a. Figure 9d presents the mean annual average minimum temperature increasing pattern with shallow D. It presented a steep rise between 1910 and 2020 with two humps at 1900 and 1980. This linear increasing pattern is due to the urban-heat-island-effect –Figure 9e presents an example of the urban-heat-island effect pattern for Hong Kong. Let us see the major trend components:

- Maximum temperature: for 1970–2020 (50 years) the trend showed 1.0°C, that is, 2.0°C/Century; for 1951–2100 global warming is 1.5°C
- Minimum temperature: for 1880–2020 (140 years) the trend showed 1.6°C, that is, 1.14°C/Century; for 1951–2100 global warming is 0.823°C
- Mean temperature: for 1910–1990 (80 years) the trend showed 1.0°C, that is, 1.25°C/Century; for 1951–2100 global warming is 0.937°C
- Mean of (maximum + minimum)/2 is (2.0 + 1.14)/2 = 1.57°C/Century; for 1951–2100 global warming is 1.18°C
- The difference between mean and mean of (Maximum + minimum)/2 is 0.122°C/Century; at global warming for 1951–2100 the difference is 0.183°C.

Discussion with reference to global warming

Figure 10a presents the global average annual temperature series for 1880–2000 given in red color and superposed on this the satellite data series in green color for about 20 years -- taken from the internet.[22] This satellite data series later was withdrawn from the internet and it was replaced with an adjusted data series that matches with the adjusted surface measured data series with steep

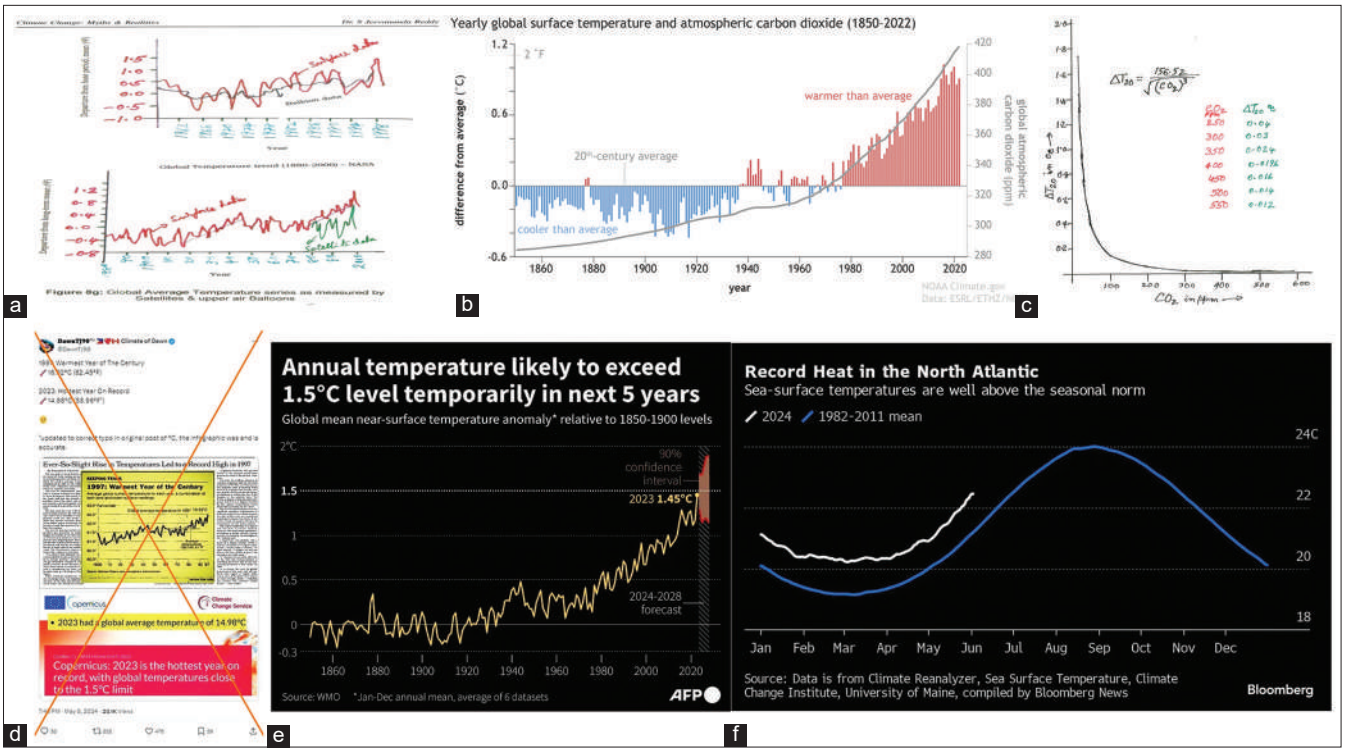

Figure 10: (a) The global average annual temperature series (bottom figure) for 1880–2000 in red color and satellite measured data series in green color, (b) Yearly global surface temperature and atmospheric carbon dioxide (1850–2022), (c) ▲T ln °C versus CO_2 in 20 ppm interval, (d) 2023 had global average temperature of 15.00°C – Copernicus: 2023 is the hottest year on record ---. (e) Annual temperature likely to exceed 1.5°C level temporarily in next 5 years (Hervé BOUILLY), (f) world sees 12th straight record-hot month and braces for more – in the North Atlantic sea surface temperature

rise, which is rarely possible. They present in reality high variations for year to year. Since 1970 the ground-based data measurements in USA were replaced with satellite data in the majority of the stations [Figure 10b]. Similar to Figure 10a [bottom curve], Figure 8f, 8g, and 8h also presented zero trend and thus zero global warming.

The satellite temperature data must be less than ground-based (surface) data. The satellite data well covers the urban-heat-island-effect as well as rural-cold-island-effect. Surface network is more in urban areas over that of rural areas and thus satellite data covers the rural-cold-island effect. Furthermore, the ocean temperatures are well covers the satellite data compared to sea surface recordings. The original satellite data series well matched [Figure 10a] showing no trend from the year 1945 onward (according to IPCC 1951 is the starting year of global warming). That means no global warming. Let us see what are the limitations in temperature and carbon dioxide (main greenhouse gas).

Reddy[22,23] presented yearly global surface temperature and atmospheric carbon dioxide for 1850–2020 [Figure 10b]. This presented unusually steep rise from 1980 to 2020 as if it is linearly increasing with carbon dioxide, which is absolutely not correct.[24]

From 1950 to 2000 the SH temperature march showed lower than that of the NH march after 1951. That means global annual average temperature, particularly, presented average of Northern and SHs averages.[24,25] The global warming component of the global average annual data series [Figure 8d] presented by 0.45/0.40°C. The SH covers more ocean/sea surface with lower temperatures and thus for the SH global warming is <0.45/0.40°C. NH covers more land area wherein land surface air temperature is higher than that of ocean temperature and thus it is >0.45/0.40°C of the global average.

Carbon dioxide

WMO compiled data relating carbon dioxide and stations recording it. The fact remains that the greenhouse gases concentrations for the past are built on indirect methods of estimation – this has inter-annual variability in the rate of increase in the atmospheric carbon dioxide (45 stations started measurements around 1960 at selected locations which are not well distributed over the globe). Total global level fossil fuels concentration is 4:1 in Northern and SHs. Source: WMO Fact Sheet No. 4, August 1989. With the non-linearly increasing population releases more carbon dioxide not the part of greenhouse gases. This is not taken into account. Global warming is not the linear function of carbon dioxide, respectively, [Figure 10a] but follow non-linear fuction.[25] NH temperature is higher than SH. This is the land and the ocean effects, respectively. Heating effect of carbon dioxide (CO^2) is non-linearly decreasing [Figure 10c] and this is expressed by the following equation (approximately).

$$\blacktriangle T = 156.52/\sqrt{[(CO_2)^3]}$$

Wherein ▲T is the °C, increase in atmospheric temperature per 20 ppm increment in CO_2.

Figure 10d presented no abrupt increase in temperature like that in Figure 10a and under the data network. It is seen from Figure 8a that the USA raw temperature data series during 1960–1990 presented below the average 60-year cycle. That is natural variability amplitude of sine curve plays important role to assess global warming if any. In Figure 10d, it presented gradual increase, but it is the same case even before 1951.

Figure 10e presents the annual temperature likely to exceed 1.5°C level temporarily in the next 5 years (Hervé BOUILLY). Before 1951 also presented a similar pattern, we do not call it as global warming, why it is so. Figure 10f presents the record heat in the Northern Atlantic sea surface temperatures are well above the seasonal norm – 2024/1884–2011 mean. In this, there is no abnormality as year-to-year variations are common.

One important point here we must look into is the urban-heat-island-effect, Figure 9d wherein showed steep rise in mean annual minimum temperature of India. The urban areas in every country increased and as a result they significantly contribute to heat-island-effect (Hong Kong heat –island-effect; Figure 9e).

Luke Howard, an amateur meteorologist in England, first recoded the heat-island-effect almost 200 years ago. Beginning in 1807, he started comparing temperatures from several sites within London with those measured a few miles beyond the city's edge, and through the years, he noticed that the city was consistently warmer. "Thus," Howard wrote in his book, "The climate of London" in 1818 under the varying circumstances of different sites, different

instruments, and different positions of the latter, we find London always warmer than the country, "the average excess of its temperature is being 1.579°." Today, the effect is more noticeable in the largest cities, average temperatures can range 5–10°F hotter than the surrounding areas.[22] That shows the possibility of maximum trend's contribution is due to urban-hear-island effect unlike IPCC proposal of less than half of the trend. In addition to this, manipulation with satellite data after 1970 onwards. All these suggests that global warming is insignificant in the temperature trend since 1951 (starting year of global warming).

CHARACTERIZATION OF SYSTEMATIC VARIATIONS IN INDIAN CYCLONES

Introduction

The word cyclone has been derived from Greek word "cyclos" which means "coiling of snake." the word first coined by Heary Piddington who worked as rapporteur in Kolkata during British rule. Cyclone is nothing but a rotational low pressure system when the central pressure falls by 5–6 hpa (hecta pascal) from the surrounding and the maximum sustained wind speed (time averaging for the sustained wind, generally IMD uses 3 min averaging for the sustained wind) reaches 34 knots (1 knot = 1.852 km/h (or) 0.5144 m/s). According scientific analysis over the cyclones, actually there are some possible conditions to form a cyclone over the sea surface. They are: sea surface temperature (26.5°), sufficient Coriolis force, low level positive vorticity, weak vertical wind shear of horizontal winds, large convective instability, low level convergence of the winds, and huge supply of moisture from the sea surface.

By following the above conditions, a cyclone will form over the sea surface. In general, cyclogenesis (birth of cyclone) occurs over the warm oceanic regions away from the equator, because the cyclones does not form near the equator due to insufficient Coriolis force which is necessary requirement for turning of winds. Coriolis force is an apparent force caused by the Earth's rotation.

The Coriolis force is responsible for deflecting winds toward the right in the NH and towards the left in the SH. This is also known as "Ferrel's Law." The deflection is more when the wind velocity is high. The Coriolis force acts perpendicular to the pressure gradient force. The pressure gradient force is perpendicular to an isobar. The higher the pressure gradient force, the more is the velocity of the wind and the larger is the deflection in the direction of wind.

If you mean tropical cyclones, it is due to their location in the tropics or subtropics surrounded by warm seas (>26°C during summer and autumn), and they are located very close to the climatological track of tropical cyclones, that is, south or south-west of the subtropical high. The best example is the Philippines. This country is located in the West Pacific ocean, the surrounding sea temperatures reach over 30°C, and the northern half of the Philippines lies very close to the average track of typhoons. The Philippines is the most heavily impacted country in the world by tropical cyclones. The sea surface temperature is one of the most important parameter among the all parameters, because it is a base to form cyclone. First, the cyclone will start as low pressure system over the sea surface due to persisting of high sea surface temperature (>26°C, because it is necessary condition to take place convection in the overlying atmosphere) and then, with the cooperation of the remaining parameters, it will be further converted as D, deep D, cyclonic storm (CS), severe CS (SCS) and very SCS and super CS based on the pressure deficit/ number of closed isobars/maximum sustained wind speed associated with the low pressure systems. The life cycle of the cyclone can be divided into four stages. They as formative stage, immature stage, mature stage and decaying stage. The formation and dissipation of a cyclone occurs through these four stages.

Weakening of cyclones in general, after just a few hours, a tropical cyclone over the land (landfall of a cyclone is the event of a storm moving over land after being over sea water) begins to weaken rapidly because the storm lacks the moisture and heat source that the sea/ocean provided. The depletion of the moisture and heat decreases the tropical cyclone's ability to produce thunderstorms near the storm center. Without this convection, the cyclones cannot survive. Another reason is friction which is higher over the land than on the sea surface. Hence, due to the insufficient supply of moisture and hear from the sea/ocean and high friction over the land than

the sea surface, the tropical cyclones weaken over the land fall.

Discussion

Typhoons and cyclone zones

Typhoons in Philippines

The Philippine Country is made up of over 7000 islands. The economy of the Philippines is one of the biggest emerging markets in the world, but many parts of the country remain very poor. On an average of 20 major storms hit the Philippines a year – Haiyan was the 25th tropical storm to enter Filipino waters in 2013. Fearsome typhoons, volcanic eruptions, and strong earthquakes. These are the three of the natural phenomena that regularly visit residents of the Philippines. The island-nation sits at a boundary of the Earth's major tectonic plates while a huge part of its territory straddles the world's notorious "typhoon belt." The Philippines is on tectonic plates on the "Pacific Ring of Fire," which means it is also prone to earthquakes and volcanic eruptions.

The Philippines straddles the "typhoon belt" [Figure 11], an area in North-west Pacific Ocean where more than 30% of the world's tropical cyclones form. This area is not only the most active in the world but also has the most intense storms globally.

The Philippines is a typhoon-prone country. Locally known generally as bagyo, typhoons regularly form in the Philippine Sea and less regularly in the South China Sea, in the months of June to September being the most active, August being the month with the most activity at least 20 typhoons are expected to hit the island nation, with five expected to be destructive and powerful. In 2013, Time declared the country as the "most exposed country in the world to tropical storms."

Typhoons typically make an east-to-west route in the country, heading north or west due to the Coriolis effect. As a result, landfalls occur in the regions of the country that face the Pacific Ocean, especially Eastern Visayas, Bicol Region, and Northern Luzon, whereas Mindanao is largely free of typhoons. The following is a list of 10 of the worst typhoons to hit the Philippines from 2009 to 2021: Typhoon Ondoy in 2009, Typhoon Glenda in 2014, Typhoon Pendring in 2011, Typhoon Pablo in 2012, Typhoon Ompong in 2018, Typhoon Lando in 2015,

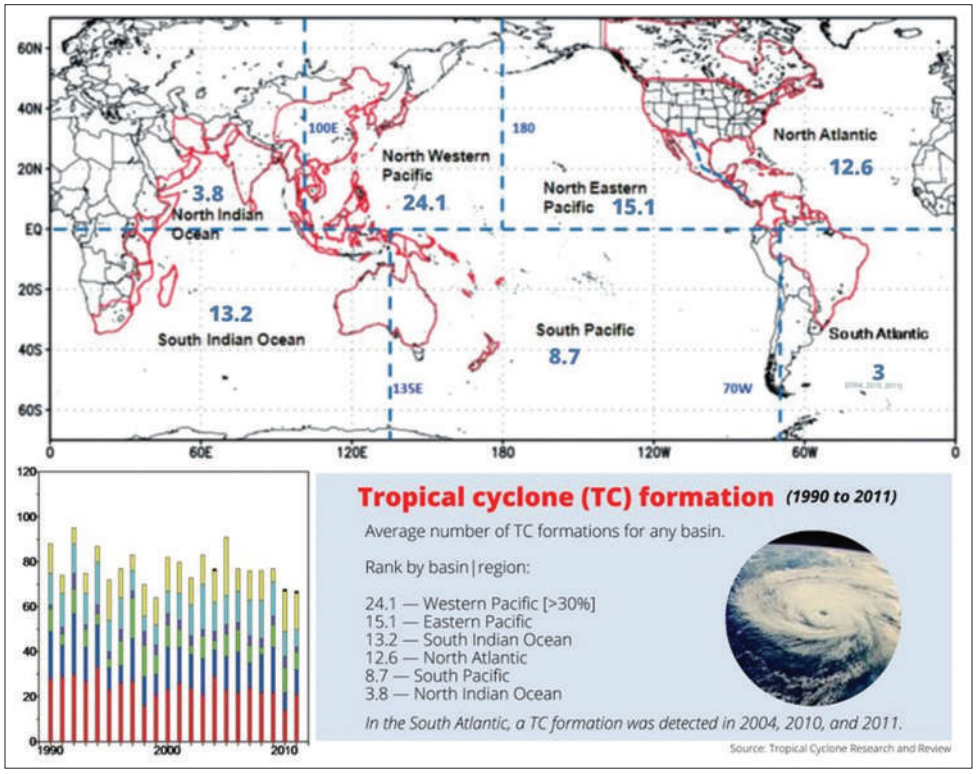

Figure 11: Intense storms: The Philippines straddles the "typhoon belt," an area in the north-western Pacific Ocean where more than 30% of the world's tropical cyclones form. This area is not only the most active in the world but also has the most intense storms globally (Source: Internet)

Typhoon Rolly in 2020, Typhoon Ulysses, Typhoon Odette in 2021, and Super Typhoon Yolanda in 2013.

Cyclone zones in India

The Indian subcontinent is one of the worst affected regions in the world. The subcontinent with a long coastline of 8041 km is exposed to nearly 10% of the world's tropical cyclones. Of these, the majority of them have their initial genesis over the Bay of Bengal and strike the East coast of India. On an average, five to six tropical cyclones form every year, of which two or three could be severe. More cyclones occur in the Bay of Bengal than the Arabian Sea and the ratio is approximately 4:1. Cyclones occur frequently on both the coasts (the West coast – Arabian Sea; and the East coast – Bay of Bengal). An analysis of the frequency of cyclones on the East and West coasts of India between 1891 and 1990 showed that nearly 262 cyclones occurred (92 of them were severe) in a 50 km wide strip above the East coast. Less severe cyclonic activity has been noticed on the West coast, where 33 cyclones occurred the same period, out of which 19 of them were severe.

Tropical cyclones occur in the months of May-June and October–November. Cyclones of severe intensity and frequency in the North Indian Ocean are bi-modal in character, with their primary peak in November and secondary peak in May [Figure 12]. The disaster potential is particularly high during landfall in the North Indian Ocean (Bay of Bengal and the Arabian Sea) due to the accompanying destructive wind, storm surges and torrential rainfall. Of these, storm surges cause the most damage as sea water inundates low lying areas of coastal regions and causes heavy floods, erodes beaches and embankments, destroys vegetation, and reduces soil fertility.

Cyclones are characterized by their devastating potential to damage structures, namely, houses; lifeline infrastructure-power and communication towers; hospitals; food storage facilities; roads, bridges and culverts; crops, etc. The most fatalities come from storm surges and the torrential rain flooding the lowland areas of coastal territories.

Figure 12 presents winds and cyclone zones in India, mainly along the East Coast and northwest parts of West Coast – very high zone. Due to this severe damage occurs for paddy crop in the rice bowl of India.

Cyclones in Arabian Sea and Bay of Bengal

Reddy[22] presented monthly cyclonic disturbances in Arabian Sea and Bay of Bengal under Ds, CSs

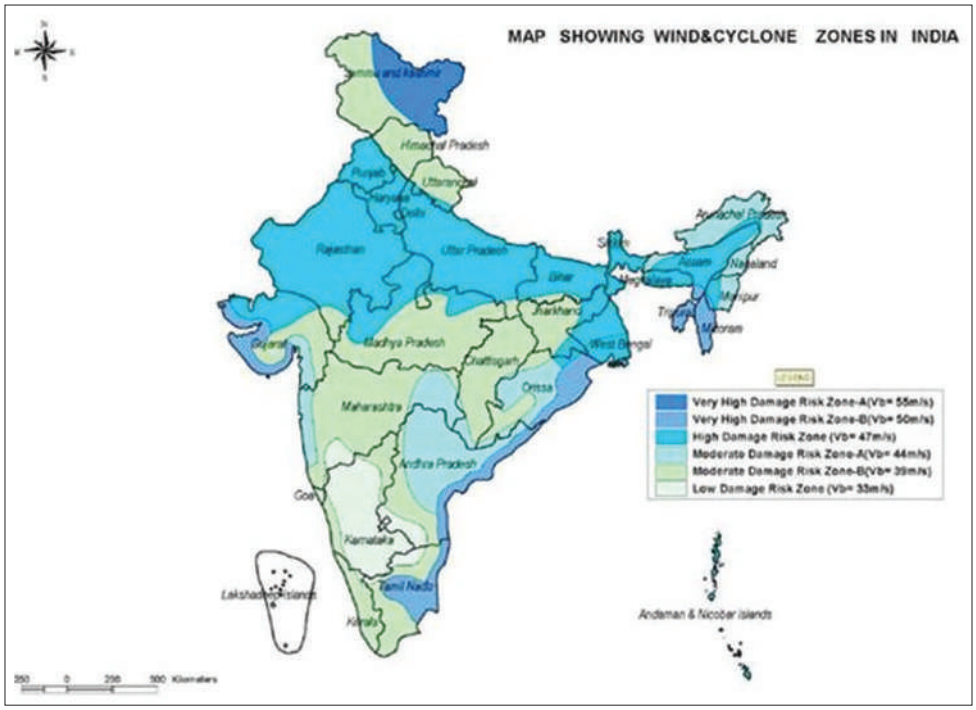

Figure 12: Winds and Cyclone zones in India (Source Internet)

and SCSs during 1891–1990. The lowest are in February and March. Table 8 presents Ds, CSs and SCS. The SCSs the highest in both Arabian Sea and Bay of Bengal in in pre-monsoon month (May – high temperature) and post-monsoon month (November – low temperature).

Bay of Bengal region cyclones per year during 1945–2000 (May to November) showed a 56 year cycle similar to SWM cycle in CA met sub-division annual rainfall. In the above the average 28-year period except 3 years, they were more than 10 per year and in the below the average 28-year period except 1 year all the years presented <10 cyclones per year [Figure 13]. We are in tropics and oceans on three sides, this creating temperature gradient that help formation of low pressure systems but they follow natural system of climate. Super CSs occurred [Figure 13] during May and November and lowest during June, July, and August and D peak here. CSs presented increasing pattern from September to November with severe cyclones reaching maximum in November.

Table 8 presents Ds, CSs and SCSs during pre-monsoon, monsoon, and post-monsoon seasons.

Figure 13 presents a weather scenario at glance over India. It presents: Seasonal (January to December) march of CA and TG met sub-divisional rainfall (mean and coefficient of variations [CVs in %] in percent) presented in left side of the figure of the average of 1891–1990 data series; also seasonal march of Ds, CSs and SCSs in Bay of Bengal are presented in the left side figure; seasonal march of Arabian Sea D, CS and SCS are shown on the right side bottom figure. The SWM rainfall of CA presented 56 year cycle and even NEM rainfall also presented 56 year cycle with opposite phase to SWM – not TG. In the left side figure it is clearly seen that the Ds are associated with the SWM (June to September); The cyclonic and SCSs are associated with pre-monsoon (April to May) and post-monsoon (October to December) periods. They are less frequent in pre-monsoon season with warm conditions and they are more frequent with the cold conditions in NEM. On the right side top figure, [Figure 13] presented number of cyclones per year in the Bay of Bengal during May to November for 1945–2000 around the average (10 cyclones per year). This pattern followed SWM rainfall pattern in CA met sub-division – 56 years cycle. In the case of above the average pattern 1 year presented below the average (<10 cyclones) and in the case of below the average most of the years, they are below the average (<10 cyclones).

The Bay of Bengal Ocean basin is notorious for generating devastating tropical cyclones, such as Nargis and the Bhola cyclone that struck Bangladesh

Table 8: Number of cyclonic disturbances during 1891–1990

Month	Number of cyclonic disturbances during 1891–1990								
	Bay of Bengal			Arabian sea			Total		
	D	CS	SCS	D	CS	SCS	D	CS	SCS
	Pre-monsoon season (April-May)								
April	08	11	10	02	04	08	10	15	18
May	32	15	35	11	15	31	43	30	66
Total	40	26	45	13	19	39	53	45	84
Monsoon [June to September]									
June	084	33	05	27	06	12	111	41	46
July	115	34	07	15	03	00	130	37	07
August	161	27	03	05	02	00	166	29	03
September	151	25	14	10	04	03	161	29	17
Total	511	119	29	57	15	15	568	136	73
Post-monsoon season (October, November, and December)									
October	104	44	34	28	12	12	132	56	46
November	55	42	53	32	06	20	87	48	73
December	37	23	19	08	04	02	45	27	21
CV%	CV%	CV%	106	68	22	34	264	131	140
CV%	CV%	CV%	185	143	47	68	900	307	253

(January–December for 100 years), D: Depressions, CS: Cyclonic storms, SCS: Severe cyclonic storms

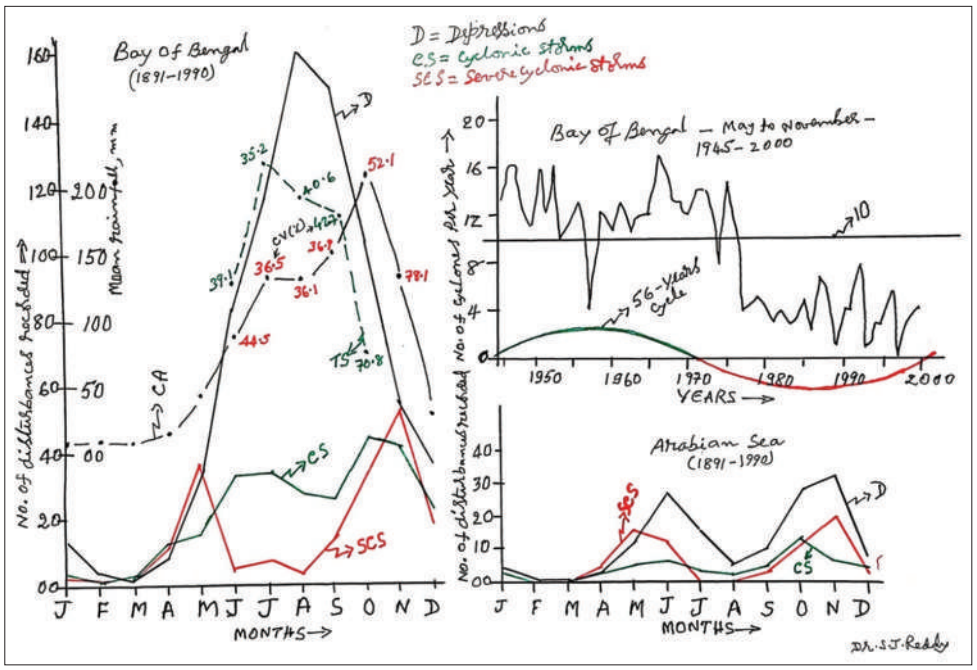

Figure 13: Number of disturbances recorded in Arabian Sea and Bay of Bengal during 1891–1990 along with rainfall pattern for the two met sub-division of Andhra Pradesh (Coastal Andhra and Telangana) along with CVs

in 1970, killing approximately 300,000–500,000 people. Tropical cyclones occur in the months of May – June and October – November. Cyclones of severe intensity and frequency in the North Indian Ocean are bi-modal in character, with their primary peak in November and secondary peak in May [Figure 13].

CHARACTERIZATION OF SYSTEMATIC VARIATIONS IN USA HURRICANES

Introduction

Peak of Hurricane Season tends to be in the mid-summer when temperatures are at their highest. Daily sea surface temperatures in the North Atlantic continue to set records, even over extraordinary warmth set in 2023, as shown in this graph [Figure 14a] from ClimateReanalyzer.org, a project of the Climate Change Institute at the University of Maine, using NOAA satellite data. The temperature variation with year to year is low during August to November that is major season for Hurricanes.

Figure 14a represents the entire NH which covers major part of land-surface area and less ocean area unlike SH – which is opposte phenomenon. With the higher temperatures with more land surface over the NH with more ocean surface with lower temperatures over SH with high humidity condition that brings down the temperature. In India pre-monsoon season temperature reaches a peak and comes down in mosoon season with humidity condition.

Even in India temperatures are higher by few degrees. This is basically due to Western Disturbances that are common to Northwestern and Northeastern parts of India in summer and wintermonths (heatwaves and coldwaves). In 2024 With cyclonic activity in Bay of Bengal, the heatwave conditions withdrew from the south by 4–6°C and after the cyclone moved toward West Bengal-Bangladesh the temperature again increased in the southeastern parts in addition to north and northeastern parts (Delhi reported more than 52°C and Nagpur more than 56°C -- though IMD rejected these values). Same is the case with Jet Stream in USA with its south to north movement. In 2024, it moved to north and created warm conditions in the south.

The warm water in the Atlantic mixes with the warm air and what you've got is a tropical cyclone -- however ocean/sea surface temperature present the cyclic pattern that control the temperature --, which builds up strength as it clears its path of destruction. Depending on its strength, a tropical cyclone in the Northern Atlantic Ocean basin is referred to as a tropical D, tropical storm,

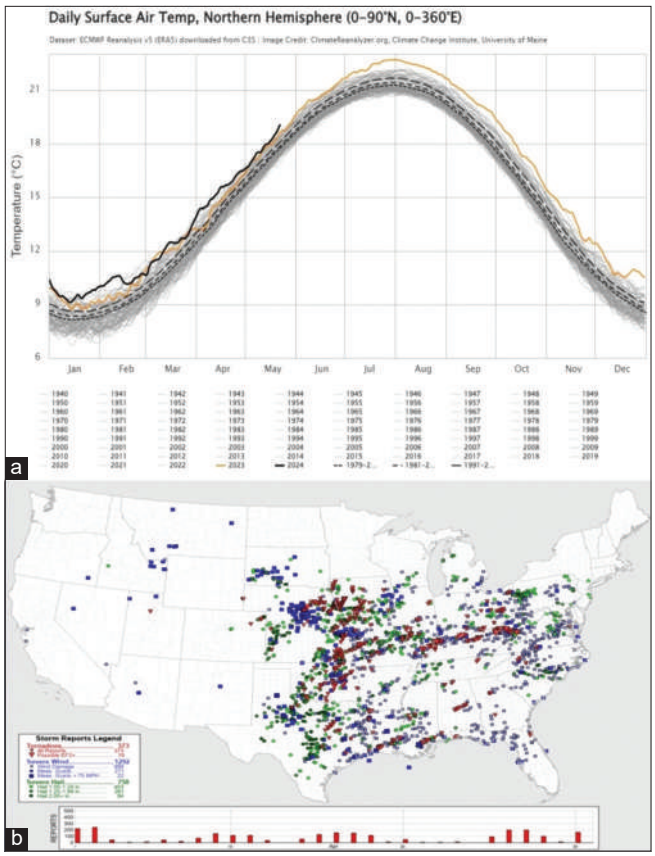

Figure 14: (a) Daily sea surface temperatures in the North Atlantic continue to set records, even over extraordinary warmth set in 2023, as shown in this graph from ClimateReanalyzer.org, a project of the Climate Change Institute at the University of Maine, using NOAA satellite data. (b) The NOAA storm prediction center showed the data of severe weather, 2004 year to date – source internet

or Hurricanes. Atlantic and Pacific Oceans present 60-year cycle in opposite phase.

Bay of Bengal Cyclones presented a 56-year cycle with no trend. Unlike Cyclones in Bay of Bengal, the Atlantic Basin/North Atlantic Ocean Hurricanes presented not only 60-year cycle but also presented steep trend. In the case of Australian sea surface, temperature presented zero trend with 120-year cycle. That means the amplitude of 120-year cycle plays rise and fall of temperature. If it follows, Atlantic Ocean the trend might come down after the completion of the third cycle.

We go on presenting saing that the heating of oceans along with global warming and or ENSO factors cause the storms birth. In the case of Bay of Bengal in India, major cyclones are reported during post-monsoon (winter season) period that is the cooling period. Hurricanes in Atlantic Basin/Ocean form in June to October with peak in August. In India that August is termed as weak monsoon month. The SWM predominantly covered by Ds [Figure 13]. The theories generalizing linking temperature rarely was successful.

Discussion

Tornedoes and hurricanes zones

Tornadoes in USA

Just in 4 months into the year-2004, tornadoes have nearly reached half of the annual average recorded over a 10-year period. April alone accounted for more than one-fourth of the annual average — approximately 1200 — tallying at least 370 tornadoes across the United States, preliminary data shows. Figure 14b presents the scatter of tornidoes this year (2024).

Hurricane zones

Tropical cyclones occur all over the world. Of greatest concern is the North Atlantic basin which includes all of the Gulf of Mexico and Atlantic Ocean coastlines of the US. Florida, in particular given it is geography, is vulnerable to tropical storms and hurricanes on an annual basis [Figure 15a and b] -- same is the case with east coast in India for the cyclonic activity.

The hurricane season in the Atlantic, Caribbean, and Gulf of Mexico runs from June 1 to November 30. Storms can and have occurred earlier (January) and later (December), but this is a very rare occurrence. Each month of hurricane season has its favored areas of formation: June, July, August, September, October, and November.

Figure 15a and b presented Hurricane season in Atlantic during 2010 and 1998. The 2010 hurricane season saw 19 named storms. The Huricane tracks conspicuously followed land scape to Atlantic Ocean. Figure 15c(i) presented the Atlantic hurricane and tropical storm activity (1944–2020). It showed a normal distriabution around 10th September. Figure 15c(ii) presents the percentage of Atlantic Tropical cyclones formations by month during 1851–2023 The peak of the season is September 10, with the most activity happening between mid-August and mid-October, according to the Hurricane Center. Nearly 95% of all major — Category 3-5 — hurricanes historically occur from August through

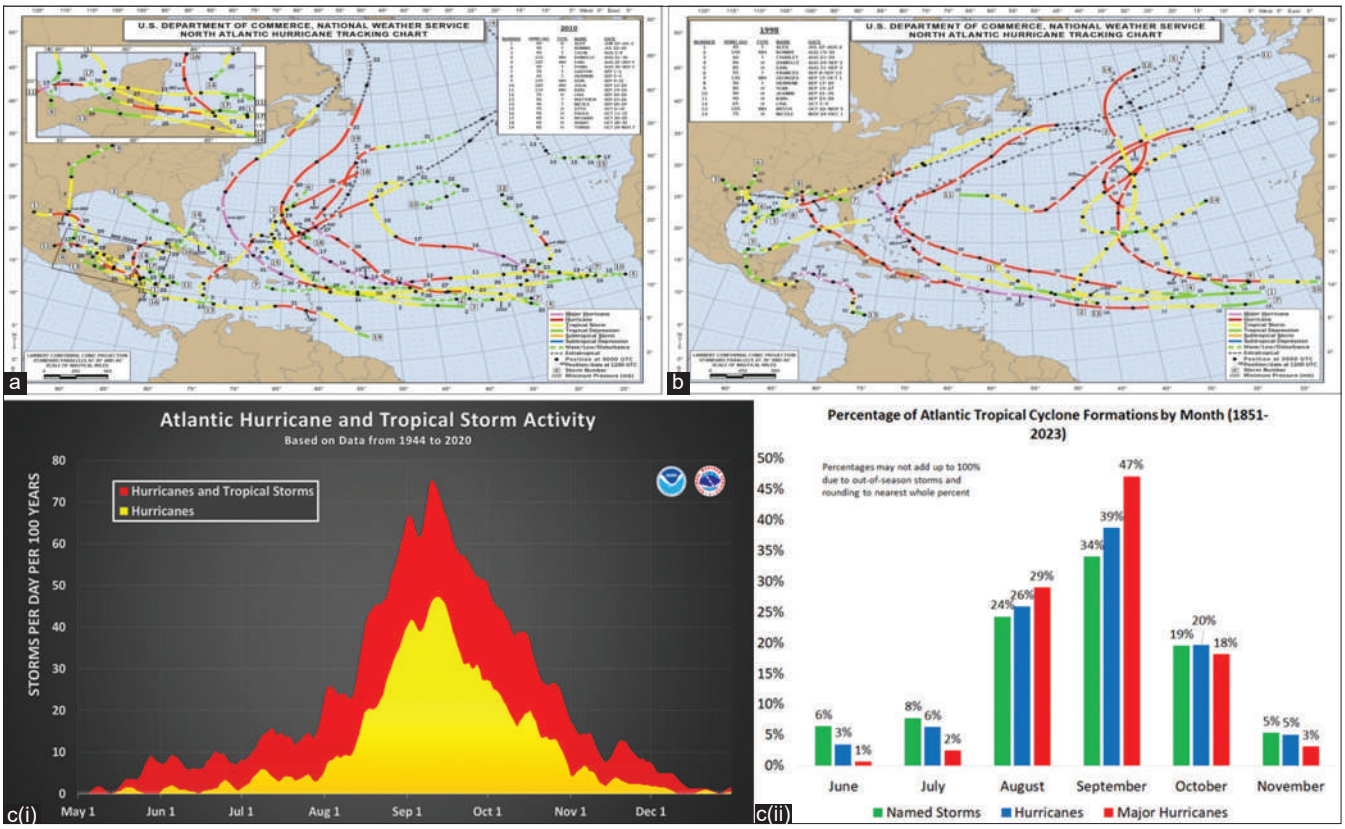

Figure 15: (a) The 2010 hurricane season saw 19 named storms-- Source Internet. (b) The 1998 Atlantic hurricane season – Source: Internet. c(i) Atlantic hurricane and tropical storm activity zone (1944–2020) – (Source: Internet). c(ii) Percentage of Atlantic tropical cyclones formations by month during 1851–2023 – Source: Internet

October, Klotzbach said. See: Daily sea surface temperatures in the North Atlantic continue to set records, even over extraordinary warmth set in 2023, as shown in this graph [Figure 14a]. It may be part of 60-year cycle.

Hurricanes in Atlantic basin

There is no difference with few exceptions between (1) Atlantic basin storms including subtropical cyclones and (2) North Atlantic Ocean Tropical Cyclones. They are all organised storm systems that form over warm ocean waters, rotate around areas of low pressure, and have wind speeds of at least 74 mph (119 km per hour).

The reason for the three names is that these storms are called different things in different places (cyclones, hurricanes and typhoons). A tropical cyclone with maximum sustained winds of 39–73 mph (34–63 knots). Hurricane a tropical cyclone with maximum sustained winds of 74 mph (64 knots) or higher. In the western North Pacific, hurricanes are called typhoons; similar storms in the Indian Ocean and South Pacific Ocean are called cyclones.

Scientists often use "tropical cyclone" as a generic term, while "hurricane," "typhoon," and "cyclone" are regional terms. The season officially starts on June 1st and ends on November 30th. Hurricanes are technically tropical cyclones, which form due to warm, moist air temperatures, which mean that the warmer and wetter the climate, the better the chance of a hurricane of some type forming.

The Atlantic basin includes the Atlantic Ocean, Caribbean Sea, and Gulf of Mexico. The Atlantic Hurricane Season starts on June 1 continue through November 30, Jessica Cameto on May 2, 2024 presented three charts relating to it. They are: Impact from tropical systems (Inland flooding, Threat of flash flooding, Stong gusty winds, Isolated tornidoes); Hurricane preparedness week (Determine your risk, Have a plan, Put together a kit) and Tropical Cyclone Forecast.

The author studied North Atlantic Ocean Historical Tropical cyclones and Atlantic Basin Storms including sub-tropical cyclones to understand the natural variability expressed as cyclic pattern and increasing or decreasing trend if any. For this purpose

the data series were collected from the internet and estimated 14-year totals in the case of Atlantic Basin Storms (with two starting point years: 1851 and 1856 like moving average technique) and presented in Figure 16a. The "average" of North Atlantic Ocean storms + Atlantic Basin storms at 10-year totals are estimated and presented in Figure 16b.

Figure 16a presented the Atlantic Basin Storms count including sub-tropical cyclones for 14-year totals as: The 14-year totals from the starting point the lowest value is 160 storms and the highest is 377 storms; that is 11–27 storms per year with the mean as 19 storms; The data series presented increasing trend; It presented increasing trend from 14-year total of 160 storms to 300 storms; that is 11–22 storms per year with the mean of 16 storms; It presented "60-year cycle" – two cycles completed and the third cycle of above the average started.

Figures 16b presented the average of North Atlantic Ocean historical tropical cyclones + Atlantic Basin storms wherein totals including sub-tropical cyclones for 10-year totals. The 10-year totals from the starting point the lowest value is 111 storms and the highest is 277 storms; that is 11–28 storms per year with the mean of 19 storms per year; The data series presented increasing trend. It presented increasing from 10-year total of 120 storms to 220 storms; that is 12–22 storms per year with the mean of 17 storms per year storms; It presented "60-year cycle" – two cycles completed and the third cycle of above the average started.

IMPACT OF ENSO ON MET PARAMETERS

On Indian Rainfall

The all-India annual average rainfall presented 60-year cycle in line with Telugu Astrological cycle. Here, the SWM season alone contributes to annual rainfall by 78.2%. In the case of AP and its three met sub-disions followed differently from All-India rainfall. AP rainfall presents 132 year cycle. Even the TG met sub-division followed this but not the other two met sub-divisions [CA and RS] but they presented 56 year cycles and SWM and NEM presenting in opposite way.

Figure 17 presents the Indian annual average rainfall and the El Nino and the La Nina conditions. In India during below the average 30-year periods of 60-year cycle in all-India average rainfall (1897–1926 and 1957–1986), the El Nino presented drought and La Nina flood conditions, respectively, in 12 and 7 years. Normal condition followed in majority of the years which can be clearly seen. Majority of the years the rainfall is between + 10% and – 10% of mean. What we really need is forecast beyond +10% and −10% limits. These represent floods and drought years. They are, respectively, 18 and 23 years.

In Table 10 presented the ENSO events during 126 years Indian SWM rainfall. Out of 126 years 84 years represented neutral condition; 49 years normal rainfall condition; 18 years El Nino condition and 24 years La Nina condition. Furthermore, these present different scales, namely, deficit, below

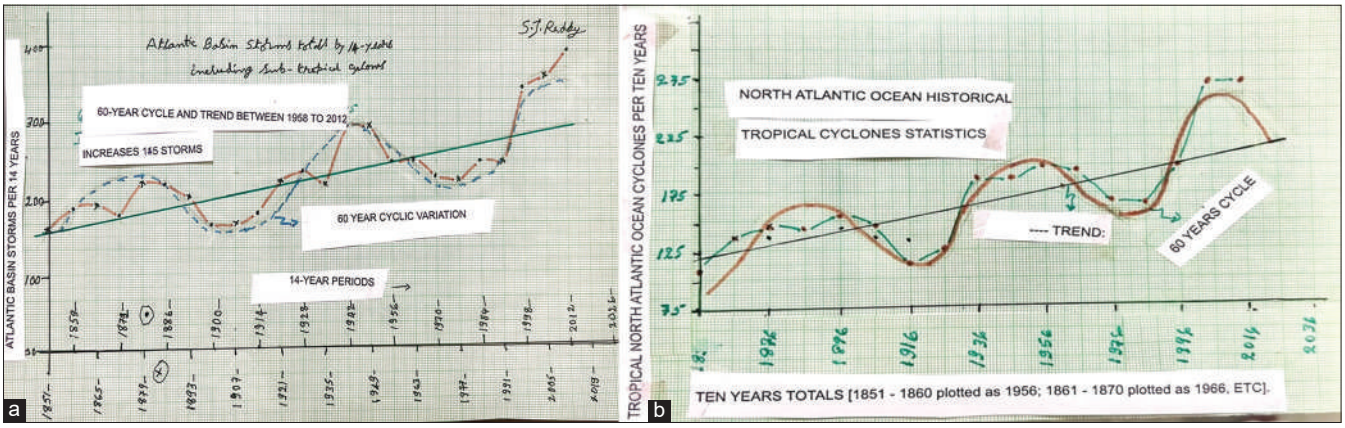

Figure 16: (a) 14-year total Atlantic basin storms wherein totals include sub-tropical cyclones presented 60-year cycle and trend of 160–300 storms of 14-year totals, (b) 10-year totals of North Atlantic Ocean + Atlantic basin average presented 60-year cycle and trend of 120–220 storms

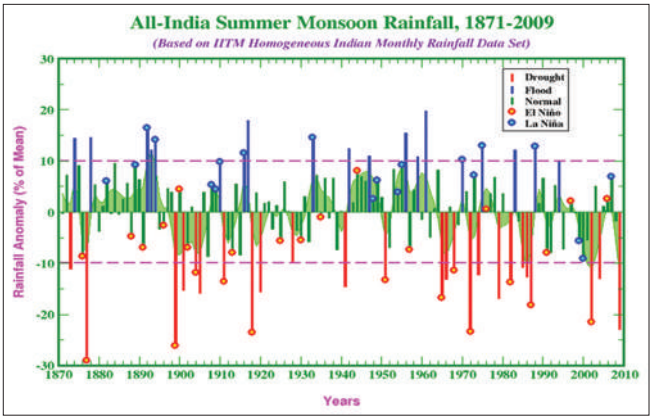

Figure 17: During below the average 30-year periods of 60-year cycle in all-India average rainfall (1897–1926 and 1957–1986) El Nino presented drought conditions (presented in 12 years) but a similar pattern with La Nina not presented floods (presented only in 7 years) – Source: IITM

Table 10: El Nino - Southern Oscillation [SO] versus Indian Southwest Monsoon Rainfall [1880 – 2006]

ENSO Events	Number of Years					
	D	BN	N	AN	E	Total
El Nino	07	05	05	00	01	18
Neutral	14	13	37	14	06	84
La Nina	00	00	07	07	10	24
Total	21	18	49	21	17	126

D=Deficit, BN=Below Normal, N=Normal, AN=Above Normal E=Excess rainfall years

normal and normal in the case of El Nino; and normal, above normal and excess in the case of La Nina. Neutral case includes all the ranges seen in the El Nino and the La Nina. Normal condition is seen in all the three states. However, these are not tallying for El Nino and La Nino in Figure 17 more particularly in El Nino periods.

On Temperatures of USA, Global, Indian and Australia

La Niña, which means "little girl" in Spanish, is a climate phenomenon characterized by the cooling of sea surface temperatures in the central and eastern equatorial Pacific Ocean. La Niña and its opposite, El Niño, as well as a neutral phase, are part of a larger climate pattern known as the ENSO. The tropical Pacific can be in either one of those three states. According to scientists, El Niño years tend to bring cold, wet winters to California and the southern U.S. but warm, dry conditions to the Pacific North-west and the Ohio Valley. La Niña tends to bring the opposite: dry conditions for the whole southern half of the country but colder, wetter weather for the Pacific North-west.

Figure 14a of Australian Annual Temperature included El Nino, La Nina, Nuetral and Volcano years. This figure has not shown any systematic impact of ENSO and Volcano events on annual temperature series for 75 years.

It is argued that global temperatures typically increase during El Nino episode and fall during La Niña. El Niño means warmer water spreads further, and stays closer to the surface. This releases more heat into the atmosphere, creating wetter and warmer air – however, it covers narrow belt along the equator. However, this system of argument countered by Western Disturbances in North-west India and by Jet stream in USA. ENSO impact factors locally are different under local general circulation patterns such as western disturbances in India during summer and winter causing heatwaves and in winter coldwaves [Figure 18a]. However the movement of heat and cold waves are modified by low pressure systems in Bay of Bengal and or Arabian Sea if any. In the case of USA, the role is played by Jet Stream – Western Disturbances and Jet Streams [Figure 18b] come under General Circulation Patterns that control temperature pattern.

Reddy and Rao[26] presented the patterns of Western Disturbance, Figure 18a presents one example. This system is modified by low pressure systems in Bay of Bengal and or in Arabian Sea. Reddy and Rao[26] presented on Western Disturbances that causes heat and cold waves. On May 24th, 2024, Times of India reported that the intensive heatwave conditions which have gripped Rajasthan for the past 10 days with mercury spiking to 49°C took nine lives. Barmer from which Balotra was carved out last year recorded 48.8°C, while Jaipur saw the maximum soaring to 47.5°C. Met office said some places in Western Rajashtan may continue to experience temperature shooting up to 49°C. Met office data showed at least 16 places in Punjab, Haryana, U.P., Gujarat and MP recorded maximum temperatures of 45°C or above, IMD said. Issued a "red" warning for Rajasthan, Punjab, Haryana, Chandigarh, Delhi, and west UP. The heat wave condition prevailed in AP and TG reduced the temperatures from 46 to

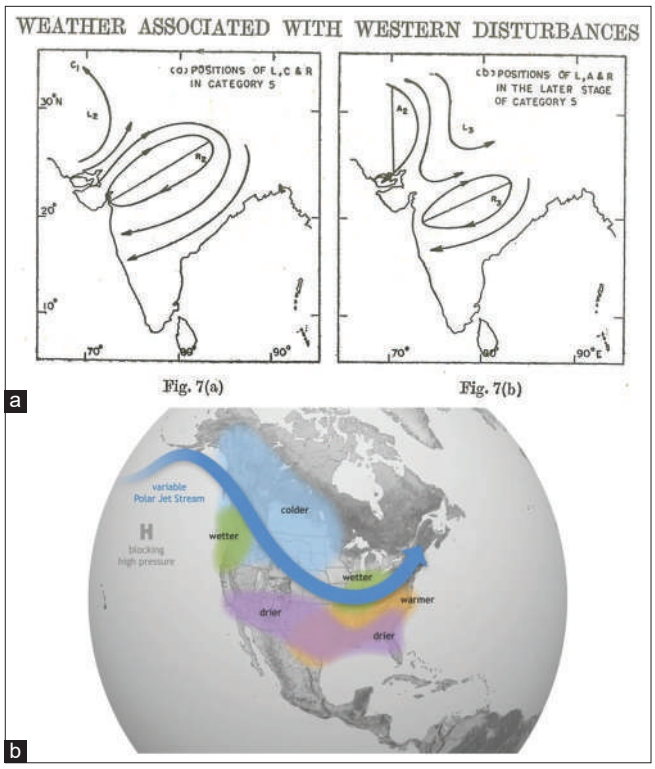

Figure 18: (a) Weather associated with western disturbances in the northwest India, (b) Position of Jet stream – act as a break for the movement of cold weather to the further southern region

36°C with low-pressure system prevailing in Bay of Bengal that counteract the heatwave winds reaching to south-east parts as presented by Reddy and Rao. [26]

A report observed that "La Niña has a notable impact on Texas weather, primarily influencing temperature and precipitation patterns. Here's how La Niña typically affects Texas, according to NOAA [Figure 18b]: (i) La Niña often brings warmer-than-average temperatures to Texas during the winter months. The warmer conditions are a result of the jet stream – similar to Western disturbances in India -- shifting northward [Figure 18b], reducing the frequency of cold air masses moving into the region. Summers during La Niña years can also be hotter than normal, with higher heatwaves and increasing demand for water and energy; (ii) La Niña is usually associated with drier-than-normal conditions across Texas, particularly in the fall and winter months. La Niña is an oceanic and atmospheric phenomenon that is the colder counterpart of El Niño, as part of the broader El Niño-Southern Oscillation climate pattern.

On Indian Cyclones

Figure 19 presents the ENSO factor and mean accumulated cyclone energy (MAE). They followed systematic pattern for some cases only. More particularly positive energy not reflected except in two cases.

The main cyclone seasons in Arabian sea and Bay of Bengal are pre-monsoon and post-monsoon seasons. The majority of cyclones formed in Bay of Bengal. Ds are covered by SWM period. The Bay of Bengal cyclones presented a natural cycle of 56-years following the SWM period of CA met sub-division's 56-year cycle. ENSO factor and MAE followed systematic pattern for some cases only. More particularly positive energy not reflected except in two cases.

It is argued that El Niño usually reduces the number of storms and hurricanes. This is a generalized notion. From this study, we can see that it is not so in the case of USA systems more particularly with Atlantic Basin Storms including sub-tropical cyclones/North Atlantic Ocean historical tropical cyclones statistics.

The warming Indian Ocean means a weakening Indian Monsoon: Monsoon is a complicated phenomenon governed by a number of variables. But one of the key ingredients in the summer monsoon precipitation is the gradient between the Surface Air Temperatures and the Sea Surface Temperatures, that is gradient is more important over magnitude of the temperature. Due to a number of components, the surface air warms faster than the sea water surface. Cooler, moisture laden winds over the Indian Ocean thus come to the Indian Peninsula and the monsoon precipitation starts. However, with an alarmingly warming in the Indian Ocean, this difference in the temperature between landmass and the sea is reduced. The sea is warming faster than the land. This warm air has more capacity to hold moisture, without precipitating it. More moisture content in the air also means rainfall more intense and a decrease in moderate rainfall. This year (2024) on set of monsoon was associated storm in seas.

A report forecasted that the El Nino may weaken by July 2024 and the La Nina start hopes raised on good monsoon. Droughts and floods form part of these to a certain extent only. Here natural variability in rainfall plays an important role. However, in pre-

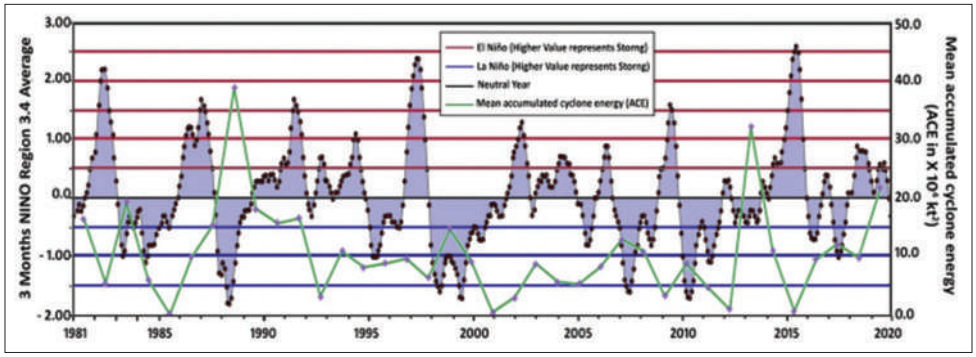

Figure 19: ENSO factor and mean accumulated cyclone energy – (Source Internet)

monsoon season in undivided AP experienced good amount of rainfall with still El Nino presence. In a week time (May 14–17, 2024], we recorded at our home around 12–15 cm of rainfall – IMD released a Bullite saying that on May 19, 2024 the onset of monsoon started over Andaman Nicobar Islands with good rains. "El Niño weakened substantially over the past month, and we think a transition to neutral conditions is imminent. There is a 69% chance that La Niña will develop by July–September (and nearly 50–50 odds by June-August) -- from Internet. Once this El Niño ends, it is likely that our spell of neutral conditions would not be a long one, with La Niña expected to develop by the late summer and last through the early winter at least." —from Internet.

This time the temperature anomalies went up to almost 3°C, making 2015 one of the strongest El Ninos in recorded history. It is significant to note that in the past 140 years, the four strongest El Nino years were 1998, 2003, 2010, and 2016. This is not seen in rainfall events. However, the onset of SWM over the Kerala Coast presented 52 year cycle similar to Fortaleza in the north-east Brasil (at the same latitude in the SH) rainfall and also related to stratospheric winds over Singapore. Figure 20a presented an example of typical El Nino and La Nina systems.

Expected El Nino patterns and impacts have played in many parts of the globe. In Africa, there has been severe drought lasting through almost the entire rainfall season. Zambia, Angola, Botswana, and Zimbabwe were likely the worst affected countries (Figure 20b) – my forecast for Beira in Mozambique is below the average (Table 6 for Beira in Mozambique the prediction is below the average for 2023–2027 and Durban in South Africa is deficit in 2010–2023 and surplus during 2024–2028). Both are correct when we look at Figure 20b.

On USA Hurricanes

It was postulated by the scientists that "An El Niño is increasingly possible by summer or fall; El Niños tend to reduce the number of storms and hurricanes in the Atlantic Basin; That was particularly the case in the most recent stronger El Niño 8 years ago; Despite that, notable U.S. landfalls can and do occur in El Niño hurricane seasons. We examined all hurricane seasons since 1966, when full satellite coverage of the Atlantic Basin began." For each of those seasons, we noted if an El Niño, La Niña, or neither was either in place or developed later in the season, based on data compiled by NOAA.

Can La Niña worsen the Atlantic hurricane season? Yes, according to the Climate Prediction Center, La Niña can contribute to an increase in Atlantic hurricane activity by weakening the wind shear over the Caribbean Sea and tropical Atlantic Basin, which allows storms to develop and intensify. It is one of the reasons forecasters have predicted a "hyperactive" hurricane season in the Atlantic basin this year, with one forecast expecting as many as 33 named storms.

An average year sees 14. Wind shear refers to the change in wind speed and direction between roughly 5000–35,000 feet above the ground, NOAA said. Strong vertical wind shear can rip a developing hurricane apart, or even prevent it from forming. This is what can happen in the Atlantic during an El Niño when Atlantic hurricane activity is often suppressed. While La Niña tends to increase hurricanes in the Atlantic, it also tends to decrease their numbers in the eastern and central Pacific

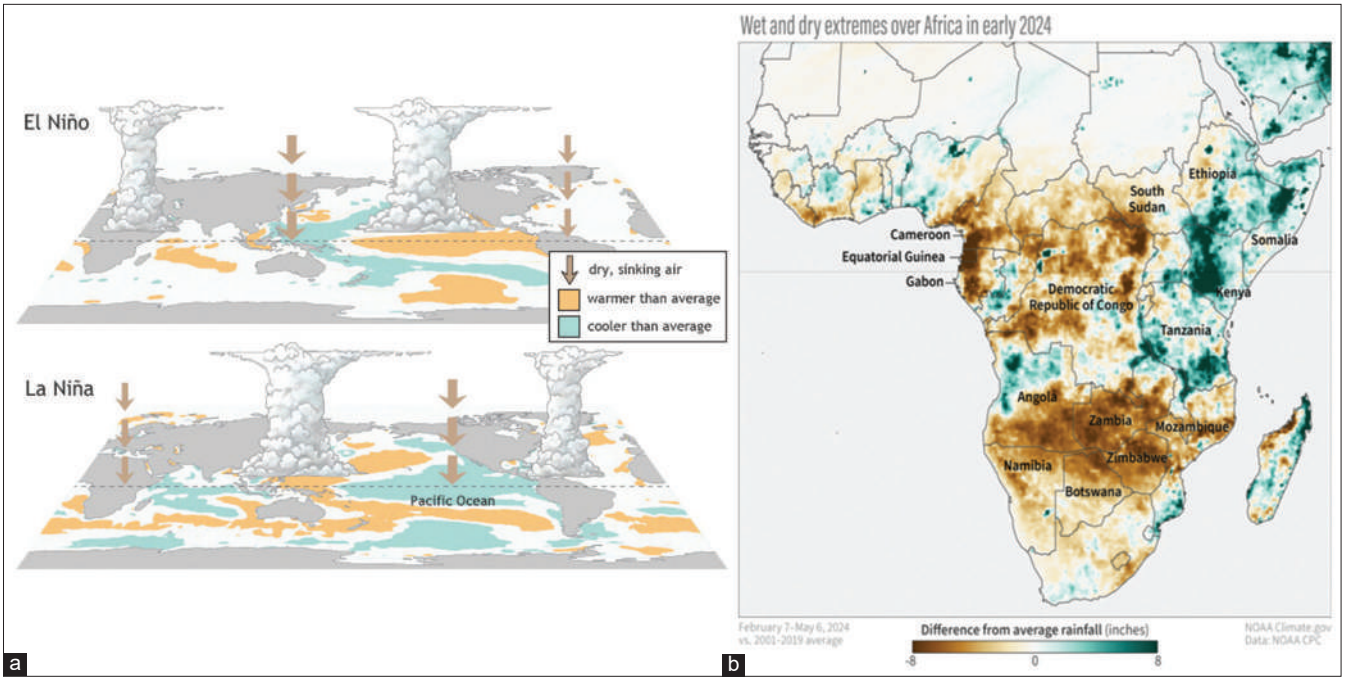

Figure 20: (a) A typical pattern of El Nino and La Nina – Source Internet. (b) Wet and dry extremes over Africa in early 2024 – (from internet)

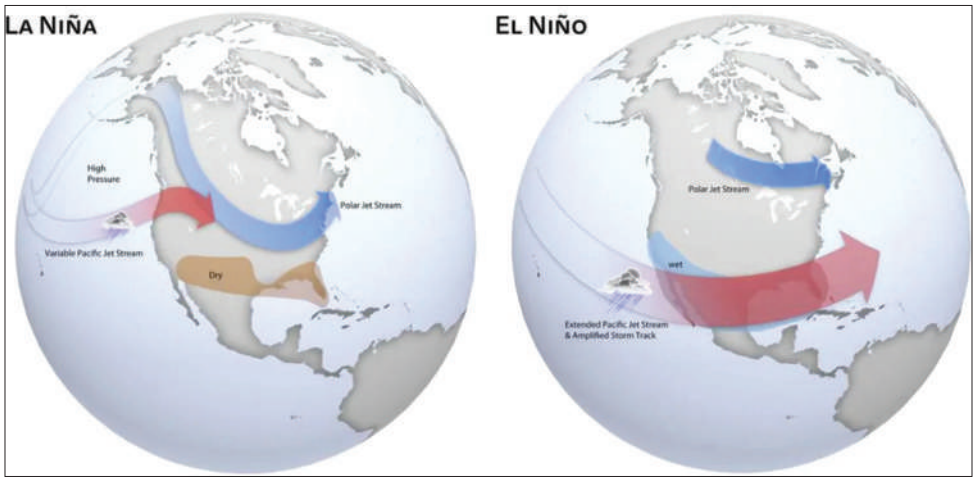

Figure 21: El Nino results in warmer ocean temperatures while its counterpart, La Niña, produces colder ocean temperatures (Source: Internet)

Ocean basins. La Niña and El Niño typically have minimal impact on U.S. weather in the summer, other than their effect on hurricanes. Winter is the one season in which they have the most impact.

Figure 21 presents La Nina tend to increase hurricane activity in the Atlantic and decrease in the Pacific and also present El Nino results in warmer ocean temperatures while its counterpart, La Niña, produces colder ocean temperatures. The inferences made from Figure 21 suggested they counter each other on the basis of ocean temperatures. One says warmer conditions of oceans and the other says colder conditions of oceans favor hurricanes occurrence or non-occurrence.

ENSO showed no impact on Figure 16a and b -- on cyclic pattern or trend but might have effected individual yearly data.

Theories on Hurricanes Forecast for 2024

Ocean heat and El Nino combine likely mean more hurricanes this year (2024) – similar to Figure 16a and b -- NOAA director Rick Spinrad said. The start of the 2024 Atlantic hurricane season is just over a

week away. However from Figure 16a and b, it is seen that "In the case of 14-year totals, the starting ending hurricanes change from 11 to 28 with the mean of 19 and with the 10-year averages they are 11–27 with the mean 19; they are with the trend, respectively, are 12–22 with the mean of 17 and 11–22 with the mean of 16 Hurricanes/storms." These results present no impact of ENSO factors. Forecasters also released their prediction for the eastern Pacific Basin, saying that a below-average season is likely. Scientists previously discovered that climate change has made extremely active Atlantic hurricane seasons much more likely than they were in the 1980s. This is because, while hotter oceans don't make hurricanes more frequent, they do make them grow more quickly and become more powerful. Global warming is a global average and thus has no significant impact at local and regional level.

In Australian data series, sea surface temperature in this study showed 120 year cycle with zero trend. That is it oscillates between the amplitude range 60 years below the average and 60 years above the average but the Atlantic Ocean two 60-year cycles completed and the third cycle above the average 30 years nearly completed with no change in trend.

Scientists also predicted that El Niño, which recently ended, will transition to La Niña, its cooler counterpart, by the summer or fall. El Niño is a climate cycle in which waters in the tropical eastern Pacific grow warmer than usual, affecting global weather patterns. During El Niño, winds in the Atlantic are typically stronger and more stable than usual, acting as a brake on hurricane formation. But if the climate cycle follows predictions and El Niño is replaced by La Niña, it could make for a particularly stormy summer. Due to this the Indian rainfall showed quite different with the El Nino, neutral, and La Nina factors.

La Niña could mean an active hurricane season. Here's what it means for Texas this summer -- summer is coming, and so is La Niña. According to the National Weather Service's Climate Prediction Centre, there is a 49% chance of La Niña developing between June and August this year, and forecasters say it will create conditions for an "above-normal" hurricane season in Texas.

A Report observed that "La Niña has a notable impact on Texas weather, primarily influencing temperature and precipitation patterns. Here's how La Niña typically affects Texas, according to NOAA:

i. La Niña often brings warmer-than-average temperatures to Texas during the winter months. The warmer conditions are a result of the jet stream – similar to Western disturbances in India -- shifting northward, reducing the frequency of cold air masses moving into the region. Summers during La Niña years can also be hotter than normal, with higher heatwaves and increasing demand for water and energy
ii. La Niña is usually associated with drier-than-normal conditions across Texas, particularly in the fall and winter months. The northward shift of the jet stream tends to divert storm systems away from the state, reducing the overall rainfall. The reduced precipitation can lead to an increased risk of drought. Texas may experience significant water shortages, affecting agriculture and water supply and increasing the likelihood of wildfires
iii. Due to warmer temperatures during La Niña winters, the likelihood of severe weather, such as snow and ice storms, is generally lower. However, La Niña can increase severe weather events like tornadoes in Texas due to enhanced instability and favorable atmospheric conditions
iv. La Niña can contribute to a more active Atlantic hurricane season. This means Texas might face a higher risk of hurricanes and tropical storms making landfall, bringing heavy rainfall and potential flooding. The NOAA predicts between 17 and 25 named storms this season, with 4–7 becoming major hurricanes classified as category 3, 4, or 5. NOAA predicts "above-normal" 2024 hurricane season in new outlook."

A report observed that "At least a dozen cities in Mexico have already broken records for high temperatures in recent days, in a pressing heatwave that has caused at least 48 deaths from heat stroke and dehydration in 2 months, according to the Ministry of Health. In the center of the country, this week, thermometers reached again 50°C. In the colonial city of Puebla [Figure 22] located about 80 km from the capital, an unusual hailstorm and rain was recorded this week that caused destruction, flooding, falling trees, and gusts of wind of up to 50 km/h, according to local authorities. "Because the third heatwave of the season will predominate

Figure 22: Despite a heatwave in Puebla, Mexico, locals were surprised after several feet of hail fell during an unexpected storm

over the national territory, maximum temperatures above 45°C are expected in Campeche, Chiapas, Chihuahua, Coahuila, Guerrero, northern Hidalgo, Jalisco and Michoacan," Conagua predicted. A similar phenomenon was experienced in City of Hyderabad in India in May 2024.

SUMMARY AND CONCLUSIONS

The principal component of "climate change" is systematic/rhythmic/cyclic variations. The present study is divided into five parts, namely, systematic variations in rainfall, temperature, cyclones, hurricanes, and the impact of ENSO on them.

Different regions of the world warm at different rates so also the rainfall. It is also different between the Hemispheres. The NH warm much faster than the SH. This is basically because more land area and less ocean area in the NH; and less land area and more ocean area in the Souhern Hemisphere. The surface Air temperatures far higher than oceans/seas surface temperatures. The oceans and their marginal seas cover nearly 70.8% of the Earth's surface which is just around three-quarters; and the exposed land occupied the remaining one-quarter of 29.2%.

Rainfall

All-India rainfall

Unlike all India rainfall wherein 78% of the rainfall on an average received during the SWM season alone, the undivided AP presented rainfall in both the SWM season and the NEM season differently and also rains are also associated with the cyclonic activity. However, the three met sub-divisions of AP presented different rainfalls in SWM and NEM in three met sub-divisions. The all-India annual average rainfall presented 60-year cycle in line with Telugu Astrological cycle. The same 60-year cycle is also seen in the SWM rainfall at all-India level.

AP rainfall

In the case of undivided AP and its three met sub-divisions followed differently from All-India rainfall. AP rainfall presented a 132-year cycle. Even the TG met sub-division followed this in addition to the 58-year cycle; but not the other two met sub-divisions (CA and RS) but they presented 56-year cycles and the SWM 56-year cycle is in opposite way to the NEM 56-year cycle. The Bay of Bengal Cyclones followed CA SWM 56-year cycle pattern. NEM rainfall is more for CA met sub-division that followed RS and the lowest in TG.

Rainfall versus river water flows

The all-India rainfall though presented 60-years cycle the undivided AP presented 132-year cycle and in both cases river water flows followed the respective cycles. For example all India rainfall 60-year cycle is seen in Brahmaputra river water flows, in northwest India, three rivers water flows and Godavari River water flows. In the case of undivided AP the 132-year, cycle is seen in Krishna river water flows. There is no trend in rainfall or water flows in the rivers.

It is observed that "The El Nino events are characterized by warm band of water developing in the central and east central Pacific", and are not a recent phenomenon. The El Nino is generally followed by a weakening of monsoon and a stronger NEM. We had a weak SWM, but NEM lashed Chennai. The Coastal AP presented 56-year cycle in the Southwest and as well in the NEMs, but in opposite phase mode. The El Nino is affecting and weakening the SWM on which India and the South Asia depend so heavily, but it is also adding to the extended warming of the Indian ocean, with long-term compounding effects. However, during 2024 May with weakening El Nino rain and cyclone influenced the east coast of India. In Summary:

- All-India annual average rsssainfall presented 60-year cycle with no trend. Same is the case with SWM Season Rainfall. The SWM Rainfall form 78.2% of the annual Rainfall

- River water flows in Northwest India, Northeast India and Central part of India's major Rivers followed all-India Annual Average Rainfall 60-year cycle pattern with no trend
- The undivided AP Rainfall and that comprised three Met (Meteorological) sub-divisions, namely, CA, RS and TG presented different patterns, namely, 132 year cycle in the case of undivided AP and Talangana met sub-division
- Krishna River Water Flows followed 132 year cycle
- TG met sub-division in addition presented 58 year cycle
- In the case of CA and RS met sub-divisions presented 56-year cycle in both the Southwest and the NEM seasons but presented in opposite form
- That is, the all-India Rainfall pattern is different from undivided AP Rainfall Patterns as the later receives rainfall in both the monsoons along with cyclonic activity in Bay of Bengal that followed the 56-year cycle of CA SWM.

Temperature

USA and global temperature

The data represents both adjusted and raw data series. Both presented 60-year cycle while the raw data showed no trend but adjusted data series presented trend. Since 1970 the satellite data is being replaced ground-based data. Satellite data well covers Sea/ Ocean (these are lower than surface data series). Temperatures are also influenced by urban heat island effect and rural cold island effect, hither this is not well covered by surface met network – both act in opposite way. This suggests the satellite data must be lower than the ground-based data, but it does not reflecting with the unusually steep rise from 2000, and may be adjusted to match the surface data series. Old satellite data showed no global warming but this was deleted from the internet.

The natural variability part of the global average annual temperature that includes both the Ocean surface (not well covered) and the land surface air temperatures data series of 1880–2010 presented 60-year cycle. The global warming starting from 1951 is 0.45°C for 1951–2100 and the global warming, for the data series of 1850–2010, it is 0.40°C for 1951–2100. In Summary:

- Different regions of the world warm at different rates so also the rainfall. It is different between the Hemispheres. The NH warm much faster than the SH. This is basically because more land area and less ocean area in the NH and less land area and more ocean area in the Southern Hemisphere (Reddy[22,23])
- The oceans and their marginal seas cover nearly 70.8% of the Earth's surface which is just around three quarters; and the exposed land occupied the remaining one quarter of 29.2%. Ocean/Seas temperature is far less than that of land surface air temperatures
- USA raw temperature data series presented 60-year cycle with zero trend but the adjusted temperature data series presented not only 60-year cycle but also showed trend basically because the starting part of the temperature was brought down
- The natural variability part of the global average annual temperature that includes both the Ocean and the surface air temperatures presented 60-year cycle. The global warming, for data series of 1880–2010, is 0.45°C for 1951–2100 and the global warming, for the data series of 1850–2010, it is 0.40°C for 1951–2100.

Indian temperatures

The Indian temperatures have been presented different patterns. The maximum temperature presented a D and this D is associated with above the average pattern of all-India annual rainfall, and thus the rainfall brought down the temperature but minimum temperature presented steep rise due to urban-heat-island effect with shallow D similar to mean temperature. Yet, the mean temperature presented global warming component of 0.53°C with sudden jump in the recent temperature in the average, maximum, and minimum temperatures. If we eliminate that part of steep rise the global warming component will be far <0.53°C – this is also applies to global average annual temperature of 0.45°C per 1951–2100. In Summary:

- Indian temperatures[24,25] of maximum and Minimum presented typical patterns. For example the:

i. Minimum temperature data series presented a linearly increasing pattern in association with urban-heat-island-effect
ii. Maximum temperature data series presented a D that coincided with the all India annual average rainfall cyclic pattern
iii. That is the D associated with the above the average rainfall pattern of 60-year cycle
iv. Indian annual average temperatures presented the global warming component of 0.53°C (this is associated with a sudden jump after 1990–2020 by 0.65°C, that means with this the global warming component will be 1.625°C for 1951–2100)
v. In Indian temperature data series one important point is that the D seen in maximum is also seen in average and minimum temperature with lesser amplitude followed mean annual all-India 60-year cycle pattern – wet period decreased and dry period increased the temperature.

Australia temperature

Australia's average annual surface air temperature anomaly for 1950–2020 presented a 60-year cycle and the inflexion point year is 1985. Here, the data are for 75 years only. It also presented 60-year cycle and similar to the global warming for 1951–2100 (150 years) 0.45°C. In this figure presented ENSO parts and Volcanos but showed no marked relation. However, the starting and ending parts of the 60-year cycle do not fit into the 60-year cycle mode. That means it follows a longer cycle than that of 60-year cycle.

The bureau of meteorology graph demonstrating how the Australia's climate has warmed since national records began in 1910. The author analyzed this data series and observed 120-year cycle for both average annual sea surface and the surface air temperatures; and the global warming trend for 1951–2100 observed zero and 0.313°C, respectively. The inflection year is 1970 for both cases.

Sea and surface air temperatures

The sea surface and surface air temperature patterns presented respective cycle amplitudes as 1.00 (−0.5–+0.5)°C and 0.90 (−0.45–+0.45)°C; however, both the data series presented zero trend, thus global warming is "zero." That means the global warming trend for the NH is more than global annual average data series global warming trend, that is >0.45°C of global average temperature with the starting data part bringing down – with the adjusted data series.

Sydney temperature

Sydney observatory hottest daily maximum temperature also presented 120-year cycle with global warming component of 2.25°C/1951–2100. Sydney's (observatory) temperature march presented the hottest daily maximum temperature for 1894–2018 with 5 point mean average 35.5°C; minimum year 1951 = 26.6°C; maximum year 2013 = 45.8°C. This showed 3.6°C trend for 120 years, that is, 3.0°C per century with the maximum temperature of 45.8°C and mean temperature of 35.5°C. The trend for 1951–2100 is 4.5°C and thus global warming for 1951–2100 is 2.25°C which is 0.65% of the mean temperature. The amplitude presents −3.5–+0.3.5°C (7.0°C), which is 2.0% of the mean. However, this is not clearly seen but replacing the trend line by horizontal line (mark at the two ends presented clear 120-year cycle). This 120-year cycle during 1944–2004 forms below the average part of the 60-year cycle; and backward from 1944 to 1985 form above the average part of the 60-year cycle. It shows sub-multiples in those periods, needs to be analyzed. The Summary:

- Australia's average annual surface air temperature anomaly for 1950–2020 presented 60-year cycle and the inflexion point year is 1985. Here the data is for 75 years only. It also presented 60-year cycle and similar to the global warming for 1951–2100 is 0.45°C
- The data relates to average annual sea surface and the surface air temperature:
  i. They presented 120-year cycle -- The inflection year is 1970 in both cases
  ii. The global warming component for 1951–2100 for the sea surface and surface air temperatures is "zero"
  iii. The Sydney's (observatory) hottest daily maximum temperature also presented 120-year cycle with no trend but there is a shift in inflection point year from 1970 to 1945 also showed sub-multiples.

Cyclones/Typhoon

The reason for the three names, Cyclones, Hurricanes and Typhoons is that these storms are called different things in different places. A tropical cyclone with maximum sustained winds of 39–73 mph (34–63 knots). Hurricane a tropical cyclone with maximum sustained winds of 74 mph (64 knots) or higher. In the western North Pacific, hurricanes are called typhoons; similar storms in the Indian Ocean and South Pacific Ocean are called cyclones. Scientists often use "tropical cyclone" as a generic term, while "hurricane," "typhoon," and "cyclone" are regional terms.

Indian cyclones

India is influenced by Arabian Sea and Bay of Bengal cyclones. Bay of Bengal Cyclones presented a 56-year cycle with no trend. The main cyclone seasons in Arabian sea and Bay of Bengal are pre-monsoon and post-monsoon seasons. The majority of cyclones formed in Bay of Bengal. Ds are covered by SWM period. The Bay of Bengal cyclones presented a natural cycle of 56-years following the SWM period of CA met sub-division's 56-year cycle. ENSO factor and MAE followed systematic pattern for some cases only. More particularly positive energy not reflected except in two cases.

Phillipine typhoons

Pacific typhoons are mature tropical cyclones that develop in the eastern and central portions of the Pacific Ocean, with the western Pacific being the most active. The Philippines has been more vulnerable in recent years with over 20 tropical storms and typhoons occurring since 2010. The Pacific typhoons season differs slightly from the Atlantic hurricane season in a few small ways. First, the season starts on May 15th and ends on November 30th. The terminology is also slightly different. Hurricanes that occur in the North Pacific are called typhoons, while those that occur in the Indian and South Pacific Oceans are called cyclones.

Cyclones

- Bay of Bengal cyclones followed the 56-year cycle of CA SWM season rainfall.
    - Now we are in the above the average (more than 10 cyclones per year – already we have seen one cyclone in May 2024) 28 years part of the cycle
    - The main cyclone seasons in Arabian sea and Bay of Bengal are pre-monsoon (Summer) and post-monsoon (Winter) seasons
    - The majority of cyclones formed in Bay of Bengal
    - Ds are covered by SWM period
    - The cyclones have peaks in May and November
- The cyclonic and SCSs are associated with pre-monsoon (April–May) and post-monsoon (October–December) periods.

Hurricanes and Tornidoes

Tornadoes

Just in 4 months into the year, tornadoes have nearly reached half of the annual average recorded over a 10-year period. April alone accounted for more than one-fourth of the annual average – approximately 1200 – tallying at least 370 tornadoes across the United States, preliminary data showed.

USA hurricanes

It is reported that "The season officially starts on June 1st and ends on November 30th of hurricanes. However, effective season starts in August with peak in September. Hurricanes are technically tropical cyclones, which form due to warm, moist air temperatures, which mean that the warmer and wetter the climate, the better the chance of a hurricane of some type forming. Hurricanes need warm, moist air to form. The water temperature near US West Coast tends to be under 75°, on an average, and hurricanes need warmer water to thrive.

The average Atlantic basin storms totals by 10-year including sub-tropical cyclones + North Atlantic Ocean historical tropical cyclone statistics presented 60-year cycliclic pattern similar to that of all-India annual average rainfall and global average annual temperature. Except rainfall the other two presented trend; while the Bay of Bengal cyclones only presented 56-year cycle similar to CA SWM rainfall. Both have no trend.

Unlike cyclones in Bay of Bengal, the Atlantic Basin/ North Atlantic Ocean Hurricanes presented not only

60-year cycle but also presented steep trend. The reasons for such a steep trend, there is no answer. Furthermore, it is not clear how long the trend move up and when the trend is going to reverse it. The Atlantic and the Pacific oceans present 60-year cycle. During 1851–2022, the lowest and the highest were 1 and 5 and 50 and 51 per year, respectively. The trend showed 118–220 storms per 10-year total series between 1856 and 2026. This data series presented cyclic variation and presented steep trend. This is also the case with 14-year totals of Atlantic basin storms. Both the sets presented 60-year cycle. In Summary:

- Figure 10 presents the Bay of Bengal cyclones per year during 1945–2000 (May–November) against the mean of 10 per year along with the 56-year cycle – curve with 1972 as inflection year on the horizontal axis. It is below the average 28 years followed by the above the average 28 years but no trend unlike that seen in Figure 16a and b – Hurricanes in USA. This pattern has no relation to ENSO factors.
- The Atlantic hurricanes season runs from June 1 through November. Storms can and do form before and after those dates
    - Reports state that both the La Niña and the El Niño tend to reach peak intensity from fall through winter, according to AccuWeather. The busiest portion of the Atlantic hurricane season occurs from August through October, with the peak being September 10
- (1) Atlantic basin storms including sub-tropical cyclones and (2) North Atlantic ocean historical tropical cyclone statistics for 1851–2023 suggests:
    - It was reported no difference in both the data series
    - The former data series at 14-year totals and both 1 and 2 combined at 10-year totals of storms presented 60-year cycles
    - Both presented steep trend
    - The lowest storms are 1 and 5 and the highest storms are 50 and 51.

General

We go on presenting saying that the heating of oceans along with global warming and or ENSO factors cause the storms birth. In the case of Bay of Bengal in India, major cyclones are reported during the post-monsoon (winter season) period that is the cooling period. In India, that period is termed as SWM with predominantly covered by Ds. The theories generalizing linking temperature rarely successful except that temperature with wet weather conditions come down but with dry conditions goes up Hurricanes in Atlantic Basin/Ocean form in June to October with peak in August.

When we say 60-year cycle, the amplitude of the sine curve plays the major role. For example for global average annual temperature presented 0.6°C of amplitude for 60-year cycle. We rarely take into account this factor when we analyze the data time series. This amplitude is seen in Australian temperature, USA temperature and Hurricanes. Even the early part of the temperature brought down scenario also the amplitude is presented.

In the case of the Australia the global warming component in surface air temperature and sea surface temperature presented "zero" global warming. That means the major component of trend in temperature is due to land-use and land cover changes – urban-heat-island-effect. However, they are localized phenomena. Due to the initially satellite data showed no trend but later it was removed from the internet. The current data showed a systematic steep rise in temperature – which rarely possible in nature. Furthermore, Sydney extreme maximum temperature presented in opposition to sea surface temperature with zero trend similar to the surface trend. It looks like SWM and NEM rainfall of undivided AP.

However, we must remember the fact that the adjusted initial period temperature is the cause for the global warming trend which can be seen from USA temperature (raw and adjusted).

ACKNOWLEDGMENT

The research is self-financed. The author expresses his grateful thanks to those authors whose work was used for the continuity of the study. The author also confirms there is no conflict of interest involve with any parties in the research study.

REFERENCES

1. Mitchel JM, Dzerdzeevskii B, Flohn H, Hofmeyer WL, Lamb HH, Rao KN. Climate Change. WMO Tech Note 79, WMO, 195 TP 100. Geneva, Switzerland: World

Meteorological Organization; 1966. p. 81.
2. Blackman BK, Tukey JW. The Measurement of Power Spectra. New York: Dower Publ. Inc.; 1958.
3. Reddy SJ. Forecasting the onset of Southwest monsoon over Kerala. Indian J Meteorol Hydrol Geophys 1977;28:113-4.
4. BRMS [British Royal Meteorological Society], USNAS [US National Academy of Sciences]. Overview: Climate Change - Evidence and Causes. Washington, DC: The National Academies Press; 2014.
5. Reddy SJ, Juneja OA, Lahori SN. Power spectral analysis of total and net radiation intensities. Indian J Radio Space Phys 1977;6:60-6.
6. Reddy SJ. An empirical method of estimation of total solar radiation. Sol Energy 1971;3:289-91.
7. Reddy SJ. An empirical method of estimation of net radiation intensity. Sol Energy 1971;13:291.
8. Reddy SJ. An empirical method for estimating sunshine from total cloud amount. Sol Energy 1974;15:281-5.
9. Reddy SJ. The estimation of global solar radiation and evaporation through precipitation-A note. Sol Energy 1987;38:97-104.
10. Reddy SJ. Dry-land Agriculture in India: An Agroclimatological and Agrometeorological Perspective. Hyderabad, India: BS Publications; 2002. p. 429.
11. Reddy SJ, Rao KR. An empirical method for estimation of evaporation from free surface of water. Indian J Meteorol Geophys 1973;24:137-52.
12. Reddy SJ, Singh S. Climate and Soils of the Semi-Arid Tropical Regions of the World. In: Presented at the Summer Institute on "Production Physiology of Dryland Crops". India: APAU and ICAR; 1981. p. 44.
13. Parthasarathy B, Mooley DA. Some features of a long homogeneous series of Indian summer monsoon rainfall. Mon Weather Rev 1978;106:771-61.
14. Reddy SJ. Climatic fluctuations and homogenization of Northeast Brazil using precipitation data. Pesq Agropec Bras 1984;19:529-43.
15. Reddy SJ. Andhra Pradesh Agriculture: Scenario of the Last Four Decades. Hyderabad, India: Jeevan Charitable Trust; 2000. p. 104.
16. Parthasarathy B, Munot AA, Kothewale DR. Monthly, Seasonal and Annual Rainfall Time Series for All-India, Homogeneous Regions and Meteorological Subdivisions: 1871-1994. Pune: IITM; 1995. p. 113.
17. Reddy SJ. Agroclimatic/Agrometeorological Techniques: As Applicable to Dry-land Agriculture in Developing Countries. Hyderabad: Jeevan Charitable Trust; 1993. p. 205. [Book Review: Agricultural and Forest Meteorology, 67:325-327, 1994]. 2nd Edition with the Same Title. New Delhi: Brillion Publishing; 2019. p. 372.
18. Reddy SJ. Climatic Fluctuations in the Precipitation Data of Mozambique during the Period of Meteorological Record. Comm. No. 39 Series Terra e Agua. Maputo, Mozambique: INIA; 1986. p. 40.
19. Reddy SJ, Mersha E. Results: Climatic fluctuations in the Precipitation Data of Ethiopia during Meteorological Record. Agrol Series 4, ETH/86/021. Addis Ababa: WMO/UNDP, NMSA; 1990.
20. Reddy SJ. Water Resources Availability in India. New Delhi: Brillion Publishing; 2019. p. 224.
21. Reddy SJ. Irrigation and Irrigation Projects in India: Tribunalas Disputes and Water Wars Perspective. Hyderabad: B.S. Publishing; 2016. p. 132.
22. Reddy SJ. Climate Change: Myths and Realities. Hyderabad, India: Jeevananda Reddy; 2008. p. 76.
23. Reddy SJ. Climate Change: Myths and Realities. Hyderabad: A.P. Akademi of Sciences; 2009. p. 167-75.
24. Reddy SJ. A note on "Weather and climate" and "global warming and climate change": Their mutual interactions. Agric Ext J 2024;8:1-19.
25. Reddy SJ. Agriculture-nutrition-foods: Impact of climate change [Temperature and Precipitation]. Agric Ext J 2024:8:1-27.
26. Reddy SJ, Rao GS. A method of forecasting the weather associated with Western disturbances. Indian J Meteorol Hydrol Geophys 1978;29;515-20.